INVITED PAPER

Ultra-Wide-Band Propagation Channels

To model and design effective UWB systems it is important to understand the distortions in each multipath component, and to be able to extract and measure channel parameters.

By Andreas F. Molisch, *Fellow IEEE*

ABSTRACT | Understanding ultra-wide-band (UWB) propagation channels is a prerequisite for UWB system design as well as communication-theoretic and information-theoretic investigations. This paper surveys the fundamental properties of UWB channels, pointing out the differences to conventional channels. If the relative bandwidth is large, the propagation processes, and therefore path loss and shadowing, become frequency-dependent, and the well-known wide-sense stationary uncorrelated scattering model is not applicable anymore. If the absolute bandwidth is large, the shape of the impulse responses as well as the fading statistics change. This paper also describes methods for measuring UWB channels and extracing channel parameters. Throughout this paper, the relationship between channel properties and other areas of UWB research are pointed out.

KEYWORDS | Channel model; propagation; ultra-wide-band (UWB)

I. INTRODUCTION

There is a general trend in wireless communications to increase the bandwidth occupied by the employed signals. This trend is caused on one hand by the constantly increasing demand for data rates—while 10 kbit/s is sufficient for speech communications, new applications like video-on-demand require 10 Mbit/s and more. On the other hand, multiple-access schemes like code-division multiple access (CDMA) require signals with larger bandwidth in order to achieve advantages like robustness to fading, improved multiple-access capabilities, and immunity to interference. Ultra-wide-band (UWB) radio pushes this trend to the limit by occupying bandwidths of 500 MHz or more (UWB with large *absolute* bandwidth) and/or using a bandwidth that is 20% or larger than the carrier frequency (UWB with large *relative* bandwidth).[1] UWB systems can thus exploit the advantages of large bandwidths to the hilt.

UWB communications has gathered great interest from the academic research community and the industry, especially in the last 15 years. This interest is due to a confluence of factors:

i) theoretical breakthroughs, especially the introduction of time-hopping impulse radio by Win and Scholtz in the early 1990s [1]–[3];
ii) new frequency regulations, in particular the 2002 decision of the Federal Communications Commission in the United States, that allow the unlicensed operation of UWB radios in the microwave range [4];
iii) advances in digital and analogue circuitry that made generating and processing of UWB signals feasible at a reasonable price;
iv) the development of new applications that required the unique features that UWB signals offer, e.g., extremely high data rates (500 MBit/s for wireless USB) [5], precise ranging and geolocation (for many sensor networks) [6], and covert high-data-rate communications (e.g., for military video transmission).

These developments in turn resulted in more than 5000 research papers on the topic, as well as the development of several communications standards based on UWB technology; for an overview and further references, see [7]–[10], as well as the other papers of this Special Issue.

Manuscript received October 23, 2007; revised February 26, 2008. Current version published March 18, 2009.
The author is with the University of Southern California, Los Angeles, CA 90089 USA (e-mail: Andreas.Molisch@ieee.org). He previously was with Mitsubishi Electric Research Labs, Cambridge, MA 02139 USA and also at the Department of Electrical and Information Technology, Lund University, Lund, Sweden.
Digital Object Identifier: 10.1109/JPROC.2008.2008836

[1]We stress that a UWB system can simultaneously have a large relative and a large absolute bandwidth.

As with any other communications system, the ultimate limits of UWB communications are determined by the propagation channel in which the system operates. Furthermore, the performance of any practical system is determined by the channel, and the design, testing, and improvement of the system hinges critically on our understanding of the propagation channels. However, three questions are habitually asked of UWB propagation researchers.

- *Why can't we use the existing insights and models for propagation channels? After all, thousands of papers have been published in the area of wireless propagation*. The main answer is "UWB channels behave in a way that is fundamentally different from conventional channels" (the basics of the differences will be explained in Section II). The differences can be due to the large absolute and the large relative bandwidth. This answer immediately gives rise to a follow-up question.
- *Why is a UWB propagation channel different from a "normal" channel? After all, a channel is a channel—it should not depend on the system operating in it*. The first answer to this question is "in principle this is correct." However, propagation research is "the art of the relevant." Wireless propagation is an extremely complicated process, and it is almost impossible to find, experimentally or theoretically, completely general descriptions and models. Rather the models concentrate on the effects that are relevant for specific systems. For example, the impulse response of UWB channels can be "sparse", i.e., characterized by a few spikes separated by times during which no significant energy arrives. This effect is a fundamental property of the channel, related to the location of scattering objects in space. However, in narrowband systems it can be—and has been—ignored: the bandpass filters in the system "smear" the signal, so that the sparseness of the impulse response is not relevant for the system. In UWB, on the other hand, the filters is wider, and thus the effect remains pertinent for the signal processing. Sections IV–VI will describe more examples.
- *Why do we care? Just build the system and try it out—this in any case is more accurate than measuring and modeling propagation channels and simulating system performance based on the models*. The answer to this argument is twofold. i) A constant cycle of redesign-field testing is an exceedingly expensive way of building communications systems. Especially for standardized systems such an approach is well-neigh impossible. ii) Even when test results show that a system does not work well in a given environment (propagation channel), this does not immediately explain *why* the problems happen. A detailed understanding of the channel and its interaction with the system, on the other hand, creates insights into possible solutions. One of the key goals of this paper is to point out the interaction between channel characteristics and system design and relate the propagation work to all the other research areas covered in this Special Issue.

UWB propagation research has been active for many years. Theoretical investigations into the interaction of short electromagnetic pulses with canonical objects have been performed since the beginning of the twentieth century [11]. However, this theoretical work was not applied to the simulations of typical wireless scenarios until the beginning of the current century [12]. Furthermore, measurements of UWB propagation channels were performed only in the late 1990s, and the first papers on statistical UWB channel models appeared only in 2001 [13]. During the last 10 years much progress has been made, though the basis of measurements on which our understanding and model parameterization is built is still somewhat tenuous.

The remainder of this paper is organized as follows. Section II covers the basic propagation phenomena in UWB channels. Next, we describe how to measure UWB channels. Sections IV and V cover the large-scale and small-scale behavior of UWB channels, respectively. An overview about deterministic channel prediction and statistical channel models follows. A summary and conclusions wrap up this paper. Consistent with the purpose of the Proceedings of the IEEE, this paper aims to give a broad overview about the particularities of UWB propagation and its interaction with other disciplines. More detailed investigations for the specialists can be found in the references, and in particular in the recent monograph [14] and the review papers [15]–[17].

II. FUNDAMENTALS OF UWB PROPAGATION

A. Multipath Propagation

A fundamental mechanism in wireless propagation is multipath propagation, i.e., the fact that the signal can get from the transmitter (TX) to the receiver (RX) via different paths and interactions [18], [19]. In order to understand this phenomenon, it is helpful to represent the electromagnetic field emitted by the transmit antenna as a sum of components that are sent into different directions (in classical propagation the components are narrow-band homogeneous plane waves, but other representations are possible too). Each of the components now propagates in space and might be reflected, diffracted, or scattered by objects (mountains, houses, trees, walls, furniture) in the environment, see Fig. 1. Each interaction process can change the direction of the components, and some interactions (like diffraction) might even split up the components into multiple new components. Components

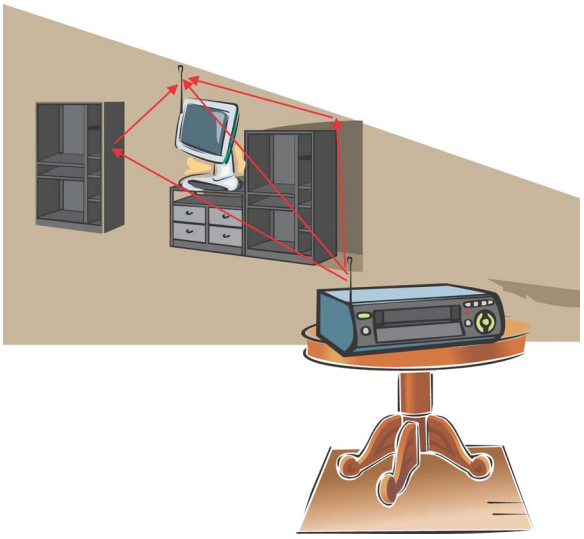

Fig. 1. ***Principle of multipath propagation.***

can take different paths, i.e., interact with different objects, before arriving at the RX antenna, and are thus called multipath components (MPCs).

Depending on the path that an MPC takes, it has a certain delay (equivalent to the length of the path that it took divided by the speed of light), attenuation, and direction of arrival. In conventional propagation research, it is assumed that interaction with environmental objects only leads to a change of direction and an attenuation of the MPC. Therefore, the signal arriving at the receiver is the sum of scaled and delayed replicas of the transmit signal and the impulse response $h(\tau)$ of the channel is (in equivalent baseband notation [18, ch. 6])

$$h(\tau) = \sum_{i=1}^{N} a_i \delta(\tau - \tau_i) \tag{1}$$

where a_i and τ_i are the gain and delay of the ith MPCs, respectively. Since TX, RX, and the interacting objects can move, the parameters in (1) are time variant; for ease of notation we do not explicitly write down this dependence. It is noteworthy that (1) can be interpreted in two ways: i) in a purely mathematical way, where we let N go to infinity (and the powers of each wave might become infinitesimally small), so that any arbitrary function $h(\tau)$ can be represented; and ii) in a physical way, where there is only a finite number of plane waves, where each wave really corresponds to a wave reflected from a faraway object. In this case, the right-hand side of (1) is only an approximate description, which ignores contributions from diffuse scattering, parts of diffracted waves, etc. [20]–[22].

Equation (1) also neglects another effect that can be especially important for UWB channels: all the interaction processes between MPCs and objects are frequency-dependent; for example, the reflection coefficient of tempered glass changes from 0.9 to 0.65 as the frequency changes from 7.5 to 10.5 GHz [23]. Therefore, the impulse response of a single MPC is not a Dirac δ function but rather a distorted pulse $\chi_i(\tau)$, where the distortion depends on the interactions that the MPC experiences on the way from the transmitter to the receiver.[2] The impulse response of the channel is consequently

$$h(\tau) = \sum_{i=1}^{N} a_i \chi_i(\tau) \otimes \delta(\tau - \tau_i) \tag{2}$$

where $\otimes$ denotes convolution.

The discussion up to now has been about propagation channels only but has ignored the characteristics of systems operating in that channel. For a further discussion we need to keep in mind that every system, including UWB, has a finite bandwidth B. As a consequence, the impulse response (1) and (2) is convolved with the impulse response of the system filter. A simplified but intuitive picture divides the time (delay) axis into "resolvable delay bins" of length $1/B$, where all contributions falling into one such bin cannot be resolved and are thus simply superposed (added up). The interaction of MPCs falling into the same delay bin gives rise to small-scale *fading*. In other words, the MPCs sometimes add up in a constructive way, and sometimes in a destructive way, depending on the relative runtimes (phases) of the MPCs. Moving TX or RX by a small distance (less than a wavelength) can turn destructive into constructive adding-up and vice versa. If a large number of (approximately) equally strong components fall into one bin, the central limit theorem becomes applicable, and the probability density function (pdf) of the complex amplitudes become complex Gaussian. This in turn implies that the pdf of the absolute amplitude become Rayleigh, and the pdf of the received power becomes a one-sided exponential (see, e.g., [18, ch. 5]).

Let us next elaborate on the distinction between UWB system with large absolute bandwidth (UWB-ABS) and UWB systems with large relative bandwidth (UWB-REL). Let a system occupy the frequency band from $f_c - B/2$ to $f_c + B/2$. Then B is the absolute bandwidth and B/f_c is

[2]Keep in mind that each MPC is weighted with the complex antenna pattern in the direction that the MPC is departing (from the TX) and arriving (at the RX), which introduces amplitude scaling and phase shifts. If the complex antenna pattern is frequency-dependent, as is often the case for UWB antennas, then $\chi_i(\tau)$ represents the convolution of the MPC distortion in the channel with the pulse distortions and weighting at the TX and RX antennas in the direction of the MPC. Furthermore, the distortions experienced by a pulse during a scattering process in the channel also depend on the direction at which the pulse is incident on scattering objects, and might thus be related to the angles at which it leaves the TX antenna and arrives at the RX antenna.

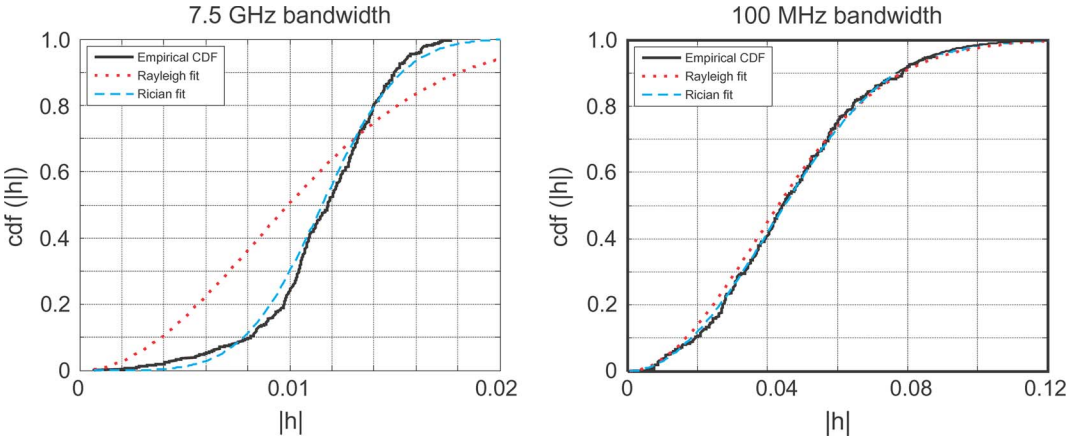

Fig. 2. *Cumulative distribution function of signal amplitude of MPCs with approximately 50 ns excess delay in an outdoor scenario (gas station) of [24]. Solid curve: empirical cdf. Dashed line: Rician fit. Dotted line: Rayleigh fit.*

the relative bandwidth, where f_c is the carrier frequency. As mentioned in the Introduction, a system is called UWB-ABS when $B > 500$ MHz and is called UWB-REL when $B/f_c > 20\%$. It is also important to note that a system can be simultaneously UWB-ABS and UWB-REL; when we speak in the following of a UWB-ABS system, we mean one that is *not* UWB-REL. Fig. 3 compares the channel impulse responses $h_K(t)$, system filter responses $h_s(t)$, and the composite impulse responses $h(t)$ for UWB-ABS and UWB-REL systems to conventional narrow-band systems. Also shown are the corresponding transfer functions, i.e., the Fourier transforms of the impulse responses.

Thus, as the system bandwidth increases, the following cases can be distinguished (Fig. 3).

- *Narrow-band systems:* these systems have such a narrow bandwidth that all MPCs fall into a single resolvable delay bin. In other words, the maximum excess delay $\tau_{max} < 1/B$; see bottom part of Fig. 3.
- *Wide-band systems:* the bandwidth is large enough that several delay bins contain MPCs. Each delay bin contains multiple MPCs, leading to fading of each separate bin. Averaging the squared magnitude of the impulse response over the small-scale fading gives the power delay profile (PDP). The most common model for the PDP is a single-exponential decay (see [18, ch. 7]). The impulse response is described by (1).
- *UWB-ABS:* when the absolute bandwidth of a system becomes very large, new phenomena occur. i) The number of MPCs falling into each resolvable delay bin decreases; therefore the fading statistics are not necessarily Rayleigh anymore. Fig. 2 shows an example of the fading statistics of a group of reflected MPCs with 100 MHz and 7.5 GHz bandwidth. ii) Not every resolvable delay bin contains MPCs, so that delay bins containing MPCs are interspersed with "empty" delay bins.[3] The resulting PDP is called "sparse." The bandwidth required for these phenomena to occur depends on the environment and need not coincide with the 500 MHz bandwidth that form the "official" boundary between wide-band and ultra-wide-band systems. The impulse response of UWB-ABS channels is approximately described by (1).
- *UWB-REL:* in these systems the duration (support) of the pulse distortion $\chi_i(\tau)$ can become larger than the binwidth (BW) $1/B$. Consequently, the pulse distortion becomes noticeable and has to be taken into account for the channel description; in other words (2) has to be used.[4] The top part of Fig. 3 shows that each separate pulse in the impulse response $h_K(t)$ is distorted, and the filtering by the system filters $h_c(t)$ does not change this fact significantly.[5] When considering the transfer function, we also find that UWB-REL systems exhibit a frequency dependence of large-scale fading and path gain. This phenomenon can be explained by the fact that frequency components with significantly different frequencies "see" different environments, since the effect of an object depends on

[3]To be more exact, it has been found that not every resolvable delay bin contains *discrete* (plane wave) MPCs, while there still might be diffuse contributions in all delay bins. Furthermore, by "empty" delay bins, we mean such bins that contain no discrete MPCs and significantly less energy than other, surrounding delay bins *on average*, i.e., the low energy level is not a result of an instantaneous fading state. Finally, we note that the obervability of empty delay bins depends essentially on the measurement SNR.

[4]Note again that UWB systems with large absolute BW can have a large relative BW. Furthermore, there can also be systems with large absolute, but small relative, BW, in which pulse distortion becomes relevant (e.g., if there is a sharp resonance or absorption line of a material in the room). In all of those cases, the more general description (2) must be used.

[5]For a UWB-ABS system (with a small relative bandwidth), the shape of the pulses in the total (filtered) impulse response is determined by the receive filters only; in other words, the pulse distortion shape $\chi(\tau)$ falls into one delay bin, so that the distortion is not noticeable after filtering.

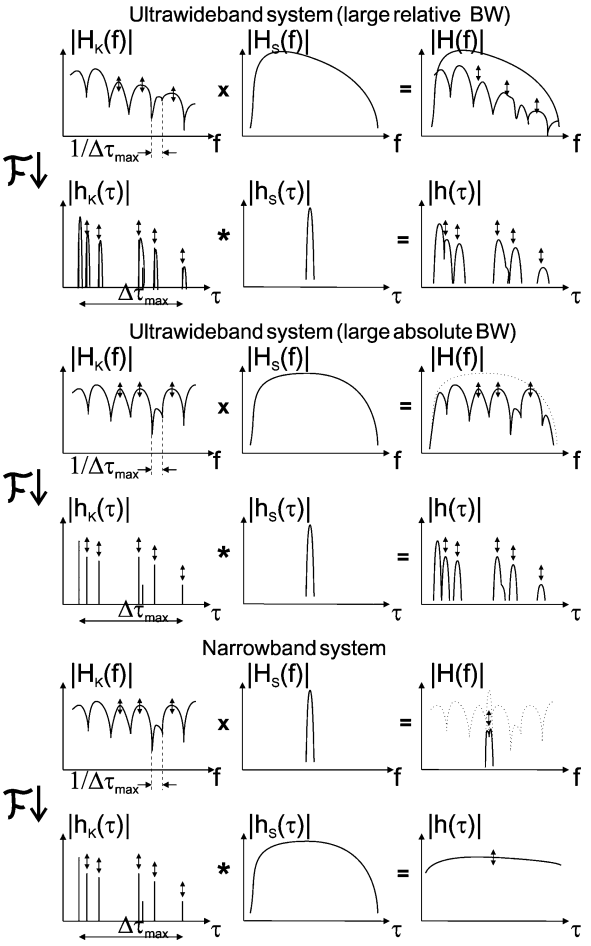

Fig. 3. ***UWB with large relative BW, and UWB with large absolute BW, and narrow-band system in time and frequency domain. $h_K(t)$ . . . impulse response of the channel alone; $h_S(t)$ . . . impulse response of the receiver filter; $h(t)$ . . . impulse response of the channel-receiver filter composite; $H(f)$ . . . Fourier transform of $h(t)$.***

its size *in units of wavelength*. For example, a signal component in the 100 MHz range can easily diffract around a car, while a signal component in the 5 GHz range is blocked by it. As a consequence of the frequency-dependence of the path gain, the wide-sense stationary uncorrelated scattering (WSSUS) model [25] cannot be applied; WSSUS requires that the fading statistics (including the mean power) are independent of the absolute frequency. Another interesting effect in UWB-REL systems is that the delay of the MPCs changes more than $1/B$ as TX or RX moves over several wavelengths [26],[6] which is the region from which "small-scale fading" statistics are extracted.[7] As a consequence, the channel statistics need not be stationary over this region—another reason for the breakdown of the WSSUS assumption.

B. Path Gain and Large-Scale Fading

Two other important phenomena in wireless propagation are path gain and large-scale fading. By *large-scale fading*, we mean that the strength of an MPC shows variations as the TX(RX) moves over distances that are larger than, say, 10λ, which is the typical small-scale averaging area.[8] The large-scale variations are caused by obstacles shadowing off (attenuating) the MPC, and are thus distinct from the small-scale fading that is caused by *interaction* between different MPCs. The effect of the shadowing is that the receiver power (averaged over the small-scale area) in areas that are at the *same* distance from the transmitter (and thus have the same path loss; see below) shows random variations. It has been shown in many measurements that for narrow-band channels, the probability density function of the received power is well approximated by lognormal distribution. Recent measurements also indicate that this remains true also for UWB channels.

The *path gain* G_{pr} describes the ratio of the received power P_{r} to the transmitted power P_{t}, averaged over both the small-scale and the large-scale fading. In this paper, we talk about path "gain" because a gain is properly defined as a ratio of received power to transmit power; note, however, that this gain is always smaller than unity (on a linear scale): the received power cannot be larger than the transmit power.[9] Path gain decreases with distance mainly due to the "thinning out" of the energy of emitted waves as they spread over a larger and larger area. We also note that it is common to write the received power and the path gain on a logarithmic scale, i.e., in decibels: $G_{\mathrm{pr,dB}} = 10\log(G_{\mathrm{pr}})$, $P_{\mathrm{r,dB}} = 10\log(P_{\mathrm{r}})$.[10] However, we stress that the averaging of the received power over the fading must be done on a *linear* scale (not in decibels).

Fig. 4 shows the distinction between small-scale fading, large-scale fading, and path gain.

The path gain, together with the transmit power and the minimum admissible receive power (which in turn depends on the actual system design), largely determines the "coverage" of a system, i.e., the distance between TX and RX for which the communication is working satisfactorily. However, an additional safety margin is required because—due to fading—the received signal quality can very greatly with location, even if the distance between TX and RX is constant. Assume now that a RX needs a power

[6]To be exact, we mean here wavelengths corresponding to the frequency at the lower band-edge; see also Section III-C.

[7]Conventional channel modeling assumes that MPCs stay within the same delay bin but minuscule changes of the delay occur and change the phase relationship between the MPCs and thus the fading.

[8]Note that the separation of large-scale and small-scale fading in UWB-REL channels is more difficult than in the narrow-band case because the conventional definition of the small-scale area (10λ) depends on the considered frequency. Finding the correct averaging areas is an important but subtle, and largely unresolved, issue.

[9]The inverse of the path gain, i.e., P_{t} divided by the average P_{r}, is denoted as "path loss."

[10]On a logarithmic scale, the path gain and path loss have the same absolute value; path gain is a negative quantity, path loss is positive.

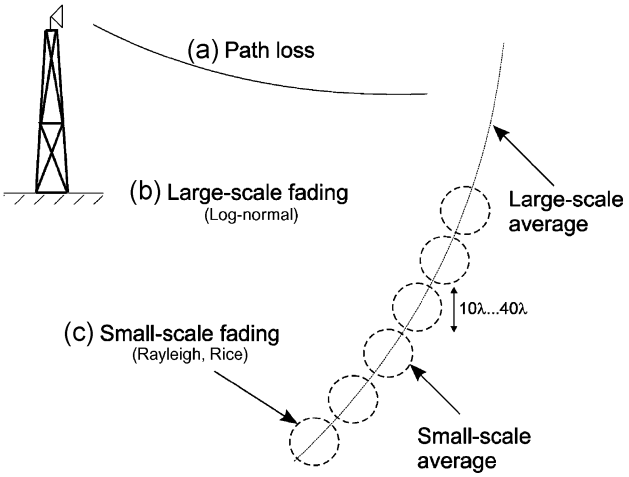

Fig. 4. *Types of receive power variation: path loss, large-scale fading, and small-scale fading.*

P_{th} to function satisfactorily. Then in a fading environment, the *mean* receiver power has to be $P_t + m_f$ and the *fading margin* m_f is chosen in such a way that the *actual* received power is greater than P_{th} in a certain percentage (typically 95%) of all locations. Clearly, the stronger the signal variation due to fading, the larger the fading margin has to be. In a UWB system, the fading margin is typically very small: first, the fading in each resolvable delay bin is less pronounced than in a conventional system (see Section V-B). Secondly, the larger number of resolvable MPCs offers a high degree of diversity: the probability that all those MPCs are in a fading dip simultaneously is extremely small.

C. UWB Communications Systems

In the following sections, we will extensively discuss the impact of UWB channels on UWB systems. We therefore give in this section a *very* brief summary of UWB transmission techniques and the associated transceivers. We can distinguish two general classes of transmission systems: time-domain (including time-hopping impulse radio and direct-sequence CDMA) and frequency-domain techniques [including orthogonal frequency division multiplexing (OFDM)], multiband techniques, and frequency-hopping). Following the mandate of the frequency regulators, this section (as well as the rest of this paper) deals only with carrier-based (also known as passband) systems. Pure baseband systems, as suggested, e.g., in [1]–[3], are not treated.

Time-domain techniques represent each transmitted symbol by one or more very short pulses; each of the pulses occupies the whole bandwidth assigned to the system. The simplest possible time-domain system is one where each pulse carries one data symbol. The duration of the pulse determines the bandwidth of the system, while the spacing between the pulses determines the data rate. Such a system is sufficient to point out some of the key effects of UWB channels on system designs.[11] The receiver for such a transmission scheme is based on a Rake receiver [27], i.e., a bank of matched filters/correlators; each correlator is responsible for receiving the pulses carried by one MPC. In the case of a single-pulse transmitter, each correlator just "gates on" when its MPC arrives and "gates off" after one pulse duration. The outputs from the correlators are then phase-adjusted so that can be added up in a constructive way. A channel characteristic that greatly impacts time-domain transmission techniques is the number of resolvable MPCs; it is not important when exactly those MPCs arrive.[12] A Rake receiver needs one correlator for each MPC it wishes to receive; therefore in a channel with a large number of MPCs, a receiver either needs a large number of correlators (which increases cost and energy consumption) or has to ignore some of the arriving MPCs, which reduces the total "useful" receive power [28].

In frequency-domain techniques the available bandwidth B is divided into a number of narrower bands, and symbols are transmitted, either in parallel or consecutively, in the different bands. The most popular such technique is OFDM, where the subbands are spaced very closely together. OFDM systems usually have a guard interval that compensates for the delay of MPCs as long as that delay is shorter than the guard interval. For this reason, the delay spread or delay window (how much energy arrives with how much delay) is the most important quantity; the number of resolvable MPCs plays a minor role for system performance.

III. CHANNEL MEASUREMENTS

A. Time-Domain Versus Frequency-Domain Measurements

The characteristics of UWB channels can be measured in either the time domain or the frequency domain, i.e., we measure either the impulse response $h(\tau)$ or the transfer function $H(f)$. While the results are theoretically equivalent and can be Fourier-transformed from one domain to the other, the practicalities of the measurement approaches are quite different [29].

The simplest time-domain measurement excites the channel by a short pulse, and the signal arriving at the receiver is recorded, e.g., with a sampling oscilloscope [30], [31]. The technique is conceptually simple but in practice it can be difficult to generate pulses that i) are short, ii) do not exhibit significant ringing, and iii) sufficiently high-powered that measurements can be made even in the

[11]Such a scheme would not be viable in a multiuser environment; a better method is time-hopping impulse radio [1]–[3].

[12]Specific arrival times of the MPCs matter only when the maximum excess delay, i.e., the time between the arrival of the first and the last significant MPC, becomes comparable to the symbol duration. In that case intersymbol interference becomes relevant, and the receiver has to contain an equalizer.

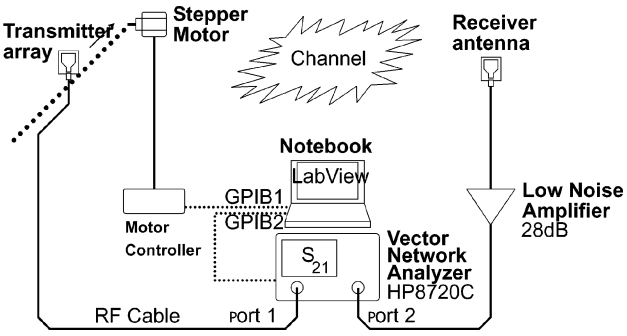

Fig. 5. ***Typical measurement setup for frequency-domain measurements.***

presence of small path gain (i.e., strong attenuation). Several of these problems can be solved by employing correlative channel sounders [32], [33]. In correlative sounders, the transmitter sends out a wide-band signal with low peak-to-average signal ratio (which is easier to generate than a short pulse containing the same amount of power), and the receiver forms the cross-correlation of the received signal with the transmit signal. If the autocorrelation function of the transmit signal approximates a delta function, then the cross-correlation at the receiver is a good approximation to the impulse response [34]. However, it is worth remembering that the delay resolution of such a system is determined by the bandwidth of the transmit signal, and generating a suitable wide-band signal with good autocorrelation properties can be even more daunting than generating short high-energy pulses.

Measurements in the frequency domain can be most easily done by means of a vector network analyzer (VNA); see Fig. 5. Those devices measure the transfer function by exciting the channel with a slowly frequency-sweeping (or stepping) sinusoidal waveform. VNAs are already available in many laboratories and can usually perform measurements over a large bandwidth. On the downside, each measurement sweep takes a significant amount of time (several seconds to several minutes, depending on measurement bandwidth and VNA model).

When deciding between time-domain and frequency-domain measurements, the following points are worth considering.

- Frequency-domain measurements tend to utilize excitation signals whose shape can be more easily controlled as the signal bandwidth becomes extremely large—in other words, vector network analyzers with 10 GHz bandwidth have transmit signals that are closer to the ideal waveform (swept- or stepped-frequency sinusoid) than the signal waveform of a pulse generator is to the ideal waveform (rectangular, Gaussian, or raised-cosine pulse).
- Inherent noise averaging in frequency-domain measurements leads to a better SNR (time-domain measurements can also improve the SNR by averaging over repeated measurements).
- Frequency-domain measurements take much longer time, thus making large-scale measurement campaigns more difficult and rendering measurements of fast time variations (e.g., due to passing people or cars) impossible.
- VNA measurements and time-domain measurements that provide information about absolute delays need a cable connection or highly accurate clocks (frequency standards) to provide trigger information. Frequency-domain measurements with scalar network analyzers [35] as well as time-domain measurements with self-triggered oscilloscopes avoid this requirement but lose some information.

B. Calibration and Antenna Issues

The measurements discussed in the previous section give the impulse response or transfer function of the combination of i) the true propagation channel, ii) the transmit and receive antennas, and iii) the measurement devices themselves. Since we are usually interested in the characteristics of the propagation channel alone, device and antenna characteristics need to be calibrated out.

Calibration of the measurement equipment alone is fairly straightforward. VNAs use a standard calibration procedure, so that the transfer function is unity when TX and RX are directly connected by cables. Similarly, we can calibrate time-domain measurement devices by measuring the impulse response when TX and RX are connected via cable and then offline eliminating this impact from the measurement results.

Elimination of the antenna effects is much more difficult. UWB antennas have complex antenna patterns that vary with frequency as well as direction [36]; furthermore, the frequency dependence of the gain might be different for each considered direction [31], [37]. In other words, an MPC is both attenuated and distorted by the antenna, and the attenuation and distortion depend on the direction of the MPC. Thus the effect of the antenna on the transfer function (or impulse response) can only be undone if the directions of the MPCs are extracted from suitable measurements [38]. Such directional measurements, as we will see in the next section, are complicated and can give rise to additional errors; to keep those errors small, the frequency dependence of the antenna patterns should be as small as possible.

Because of those practical difficulties, many measurements in the literature do not perform an antenna calibration at all, i.e., they present measurement results for the concatenation of a specific antenna with the channel that they have measured. Other papers perform an approximate calibration, ignoring the frequency dependence of the antenna patterns. When interpreting measurement results, it is very important to keep in mind what calibration procedures have been used.

C. Directional Measurements and Parameter Extraction

Directional information about MPCs is required for calibrating out antenna effects, as discussed above. Furthermore this information is also vital in the context of multiantenna systems. Directional information is usually obtained from antenna array measurements, i.e., measurements by a number of closely spaced antennas. The measurements can be done either with a real array [39] or a synthetic array, i.e., a single antenna mechanically moved to different positions. The location of the antennas (measurement points) should be spaced at most $\lambda/2$ apart, in order to avoid ambiguities of the measured directions of arrival [40]. For UWB, unambiguous resolution of the directions at all frequencies requires that the measurement points are at most $\lambda_u/2$ apart, where λ_u is the wavelength at the upper band-edge.

Array measurements allow the extraction of the parameters (including directions) of the MPCs. A number of different algorithms types have been proposed.

- *Maximum-likelihood parameter techniques*. The most popular such algorithm, the SAGE algorithm [41], is an iterative, approximate implementation of a maximum-likelihood estimator. During each iteration, it estimates one parameter and cancels its contribution from the overall impulse response or transfer function. In its original form, SAGE is based on the narrow-band assumption, though attempts to generalize it to the UWB-REL case have recently been made [42]–[44].
- *Correlation-and-cancellation*, like the CLEAN algorithm [31] and extensions [24]. The basic premise of these algorithms is that the observed signal is a sum of pulses with known shape. The algorithm then first finds the largest pulse by correlating the received signal with the pulse shape. The contribution of the thus-identified pulse is subtracted from the total signal, and the process is repeated until the energy of the "cleaned-up" signal falls below a threshold. Note that this class of algorithms is rather similar to the SAGE algorithm, as both perform cancellation of already-estimated components, though the implementation details are somewhat different.
- *Extraction of azimuthal spectra by transformation techniques* [45], [46]. In this approach, a Fourier transformation of the signals received a uniform linear arrays is used to obtain the directional spectra of the signals.
- *Orthogonal correlators* [47] and least squares estimation [48].

The above algorithms are generalizations of narrow-band algorithms, and there are open questions about under what circumstances the generalization is possible, and whether additional processing steps are required. The key problem of any estimation algorithm is the determination of the pulse distortion $\chi_i(\tau)$, or, equivalently, the frequency dependence of the transfer function of each MPC. It is required for any of the above algorithms to work, but it is difficult to distinguish between a distorted pulse extending over two delay bins and two undistorted MPCs that fall into adjacent delay bins. Many aspects of directional estimation in UWB thus remain open research problems.

The extraction of the *statistics* of the small-scale fading also suffers from some problems that are particular to UWB. In order to extract the small-scale fading statistics of UWB channels, multiple measurements have to be taken within an area where the large-scale fading (shadowing) is constant, but the fading in the resolvable delay bin changes. In order for the measurement results to be approximately uncorrelated, the measurement points must be spaced half a wavelength (the wavelength at the *lower* band-edge) or more apart. For UWB-REL systems, this is in contrast to the criterion for measurements that allow the extraction of directional characteristics, where the measurement points must be spaced at most half a wavelength (at the *upper* band-edge). An additional difficulty arises from the fine delay resolution of UWB systems: when the measurement location moves over several wavelengths, the MPC can fall into a different delay bin, as discussed in Section II-A. Thus the amplitudes of a given delay bin do not reflect the interaction of a given (constant) ensemble of MPCs,[13] leading to a possible violation of the conditions for WSSUS [25].

IV. LARGE-SCALE CHARACTERISTICS

A. Distance Dependence of Path Gain

As discussed in Section II, the path gain is a measure for the average attenuation of the signal from TX to RX. It obviously depends on the distance between TX and RX and, together with the transmit power, determines the range of a wireless system: for distances beyond a certain range, the received signal strength becomes so weak that proper reception is not possible anymore.

For the distance dependence, the classical power law

$$G_{\mathrm{pr}}(d) = G_{\mathrm{pr},0} - 10n\log_{10}\left(\frac{d}{d_0}\right) \tag{3}$$

can be used, d_0 is the reference distance, $G_{\mathrm{pr},0}$ is the path gain at the reference distance, and n is the propagation (path gain) exponent. For free-space propagation, $n = 2$ is valid, but note that *all* positive values of n are physically meaningful (we just require that the received power is not larger than the transmit power). The path gain exponent depends on the environment in which the system operates; it can range from less than one in corridors with line-of-sight (LOS) to seven in some indoor situations with severely blocked propagation. Typical values for LOS are on the order of 1.5, and for non-LOS on the order of 3–4 [49]–[55].

[13]Runtime corrections can be applied, but only if the direction of the MPCs is known.

A more refined model of the path gain treats the path-gain exponent as a random variable, where variations can occur from house to house (for indoor environments) [56], [57] or, for outdoor channels, between locations that are widely separated [58].

Large-scale fading, as discussed in Section II, shows a lognormal distribution, with a variance of typically 1–2 dB (LOS) and 2–6 dB [non-LOS (NLOS)], depending on the environment [51], [53]–[55], [59]. Similar to the path-gain exponent, also the shadowing variance can be modeled as random variable [57], [60].

Path gain and shadowing have a key impact on the coverage and interference characteristics of wireless systems. Usage of different path gain models can greatly change the conclusions about a system. System manufacturers that want to demonstrate good coverage by their systems often use a path-gain model with a deterministic $n = 2$; this assumption might be valid over very short distances; however, such a value is wildly optimistic in non-LOS situations. Frequency regulators also tend to assume a very small n, but in that case it serves as a *worst* case, namely, that UWB emitters can cause interference even at large distances. Note also that desired signal and interference can have different path-gain exponents. For example, both high and low values of n occur when n is modeled as a random variable. This leads to especially challenging scenarios, as, on one hand, the "reliable" coverage distance (i.e., the distance up to which 95% of all locations receive sufficient signal strength) is small due to the high values of n, while the worst case interference scenarios occur whenever n takes on a low value.

B. Frequency Dependence of Path Gain

In a UWB-REL systems, the path gain can become frequency dependent. Thus, when looking at a frequency-domain transmission technique, we find that the achievable range is smaller at higher frequencies, where the path gain is smaller; alternatively, the high-frequency subbands can carry less information. To formalize this concept we thus consider the path gain in different frequency bands, each of which has a small relative bandwidth Δ, so that diffraction coefficients, dielectric constants, etc., can be considered constant within that bandwidth (see also [61], [62])

$$G_{\mathrm{pr}}(d,f) = E\left\{ \int_{f-\Delta f/2}^{f+\Delta f/2} \left| H(\widetilde{f},d) \right|^2 d\widetilde{f} \right\} \qquad (4)$$

where the expectation is taken over both small-scale and large-scale fading and d is the distance between TX and RX. It is commonly assumed (and supported by recent measurements [63]) that the distance-dependence and frequency-dependence of the path gain are independent of each other, i.e., $G_{\mathrm{pr}}(d,f) = G_{\mathrm{pr}}(f)G_{\mathrm{pr}}(d)$. The frequency dependence of the path gain is in turn determined by the frequency dependence of all the propagation processes that the MPCs undergo, including free-space transmission, reflection, and diffraction. It has been observed that $G_{\mathrm{pr}}(f) \propto f^{-2\kappa}$ fits well with measurements, where κ typically lies in the range of 0.5–1.5 [64]–[68][14]; alternative models are described in [70] and [71]. Note that $\kappa = 1$ corresponds to the classical "free-space path loss"; higher values can be explained by the fact that diffraction losses increase with frequency. Measurements suggest that the shadowing variance is approximately independent of frequency [53].

V. SMALL-SCALE CHARACTERISTICS

In this section, we first discuss the fading of the resolvable MPCs. We then turn our attention to the statistics of the arrival times of the MPCs and how the arrival times are linked to the average powers of the (resolvable) MPCs. Lastly, we discuss the statistics of the angles at which the MPCs depart and arrive from the TX and at the RX, respectively. All those considerations concentrate on UWB-ABS, unless otherwise noted.

A. Fading

Despite the high temporal resolution of UWB systems, there is still an appreciable probability that several MPCs fall into one resolvable delay bin and add up there; in other words, there is fading even in UWB. The difference to a conventional system lies mainly in the number of MPCs that fall into one bin. This number is influenced by i) the environment: the more objects are in the environments, the more MPCs can occur—for example, residential environments tend to have fewer MPCs than industrial environments [67]; ii) the measurement bandwidth: clearly, a larger bandwidth, and thus a shorter duration of a resolvable delay bin, reduces the number of MPCs per bin; and iii) the delay of the considered bin: for larger excess delays, there are more feasible paths causing this particular delay. Thus, fading depth increases with increasing delay [30], [72]. Depending on these factors, a Rayleigh distribution of the amplitudes might or might not be suitable. If this is not the case, a number of alternative distributions have been suggested.

- *Nakagami distribution* has been suggested in [30] and was also confirmed in [32] and [66] for bins with large delays.
- *Rice distribution* has been suggested by [66] and [72] for bins with small delays in LOS situations. Reference [33] found it to best fit measurement results in an office environment.
- *Lognormal distribution* was introduced by [73]. This approach has the advantage that the fading statistics of the small-scale statistics and the large-scale variations have the same form.

[14] $\kappa = 1.3$ was observed in the context of cellular systems [69].

Other distributions have been suggested as well [71], [74], [75] but are not in widespread use. The agreement of a number of different distributions with measurement results can be tested by means of information-theoretic criteria to identify the distribution that fits best [33].

Another important point is whether the fading in adjacent delay bins is correlated. Reference [71] found that components immediately following the LOS have a high probability of having the same polarity as the LOS. Reference [30] found that the fading of adjacent delay bins was uncorrelated (for a measurement bandwidth of less than 1 GHz; [33] found only weak correlation for bandwidth up to 3 GHz in the microwave range. Strong correlation has been found in body-area networks [76], [77].

B. Delay Dispersion

1) Arrival Times and Clustering: Arrival times of MPCs are related to the location of the interacting environmental objects. Especially if each MPC experiences only a single interaction on its way from TX to RX, then the location of the interacting object uniquely determines the excess runtime by means of a simple geometrical relationship. It has been shown that if objects are distributed uniformly in a plane, then the arrival statistics of the MPCs are random variables following a Poisson distribution (with arrival rate β)[15]; in other words, the interarrival times between MPCs are exponentially distributed [78].

In most indoor environments, however, objects are not distributed uniformly in space but rather are *clustered*. Roughly speaking, a cluster is a group of objects that are close together and are separated from other objects by a considerable distance. A table with surrounding chairs, or books on a shelf, are examples for objects that are present in clusters. The clustering of objects can be, in a first approximation, translated into clustering of MPCs (a more detailed definition of clustering also takes the properties of MPC in the angular domain into account [79], [80]). Thus the impulse response is written as

$$h(\tau) = \sum_{l=0}^{L} \sum_{k=0}^{K} a_{k,l} \delta(\tau - T_l - \tau_{k,l}) \tag{5}$$

where $a_{k,l}$ is the tap weight of the kth component in the lth cluster, T_l is the delay of the lth cluster, $\tau_{k,l}$ is the delay of the kth MPC relative to the lth cluster arrival time T_l, and K is the number of MPCs within a cluster. L is the number of clusters. Formally, (5) does nothing but split a summation into a double-sum, and the reader might wonder what the advantage in this is. The reasons are that i) it is easier to establish a relationship between the physics of the environment and the impulse response and ii) the statistics of the MPCs *within* a cluster can be described in a simple manner, and the statistics of the clusters themselves can be easily described as well; in contrast it is very difficult to describe the joint statistics of *all* the MPCs.

The popular Saleh–Valenzuela (SV) model [81] (see Fig. 8) suggests that the cluster arrival times T_l are Poisson distributed variables, with interarrival rate Λ, i.e., the interarrival times of the clusters are exponentially distributed. $1/\Lambda$ is typically in the range of 10–50 ns [54], [59], [70], [82]. The SV model furthermore models the interarrival times of the paths within one cluster as a Poisson process with arrival rate β. A generalized Poisson-mixture model was introduced by [55] and [83] and also used in the standardized IEEE 802.15.4a model [67]. Parameterizations in different environments are given in [31], [67], and [83]–[86].

Clustering is not a phenomenon that exclusively occurs in UWB channels; as a matter of fact, the SV model was not established with UWB in mind. Depending on the environmental parameters and the bandwidth of the system, a variety of scenarios can occur.

- Unresolvable clusters: if the bandwidth is very small ($B < 1/\tau_{\max}$), neither clusters nor MPCs are resolvable.
- Resolvable clusters but unresolvable MPCs: if $\Lambda < B < \beta$. This case has often be observed in outdoor environments even when the bandwidth is only on the order of 1 MHz. However, in indoor environments, bandwidths of 10 MHz or more are necessary for this case to occur.
- Resolvable MPCs: if the bandwidth is sufficiently large ($B > \beta$), then the MPCs can be resolved. Resolvable delay bins containing MPCs are interspersed with delay bins that contain no MPCs, so that the impulse response becomes truly sparse.

Fig. 6 shows the effect of filtering with a 500 MHz filter. It is clear that while the impulse response is somewhat smeared by the filtering, it is still sparse.

The number of clusters depends both on the environment and the measurement bandwidth [87] and typically lies between 1 and 5, though values higher than ten have also been observed [32], [54], [55], [57], [59], [88]. L can be modeled as fixed [89] or as a stochastic variable [82].

2) Delay Dependence of Power of MPCs: Equation (5) is fairly general. It can be used in conjunction with MPC arrival times that can either be regularly spaced or random. It can also be used in conjunction with different models for the power contained in the various clusters. The most common model for the power delay profile of each cluster is a one-sided exponential decay

$$E\left\{|a_{k,l}|^2\right\} \propto \Omega_l \exp(-\tau_{k,l}/\gamma_l) \tag{6}$$

[15]It is standard in the literature to abbreviate the arrival rate as λ. However, in order to avoid confusion with the wavelength, we use β in this paper.

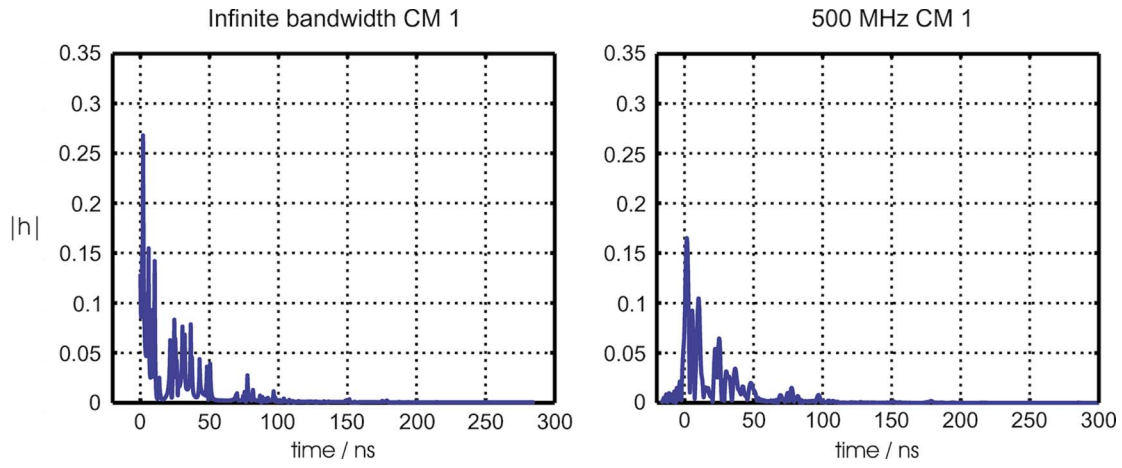

Fig. 6. *Effect of filtering on impulse response. (Left) Unfiltered impulse response in indoor environment; (right) filtered with 500 MHz bandwidth rectangular filter.*

where Ω_l is the integrated energy of the $l-$th cluster and γ_l is the intra-cluster decay time constant. The cluster powers, averaged over the large-scale fading, follow an exponential decay with a different decay time constant. The intercluster decay time constant Γ is typically around 10–30 ns, while widely differing values (between 1 and 60 ns) have been reported for the intracluster constant γ; see, e.g., [54], [59], and [82].

Another important special case is when $L = 1$; this recovers the classical single-exponential decay model. Other measured cases include the following.

- Single-exponential decay $(L = 1)$ with strong first component [30]: this shape was observed in indoor environments with a low carrier frequency, so that the first arriving MPC was strong even if the direct line-of-sight was blocked.
- Single-exponential decay $(L = 1)$ with random variations. The PDP is not strictly monotonic but shows a "fine structure," i.e., the PDP can be modeled as a purely exponential decay multiplied by a lognormally distributed random variable [57], [90].
- Soft onset: in some environments the first arriving MPC does not carry the largest energy. Rather, the PDP slowly rises to a maximum (typically 20–50 ns after the first MPC) and then decays again [51], [67]; compare Fig. 7.

Comparisons among various models were done in [91].

3) System Implications: The characteristics of the delay dispersion have great impact on the design of the receivers as well as on the performance of ranging devices. In the

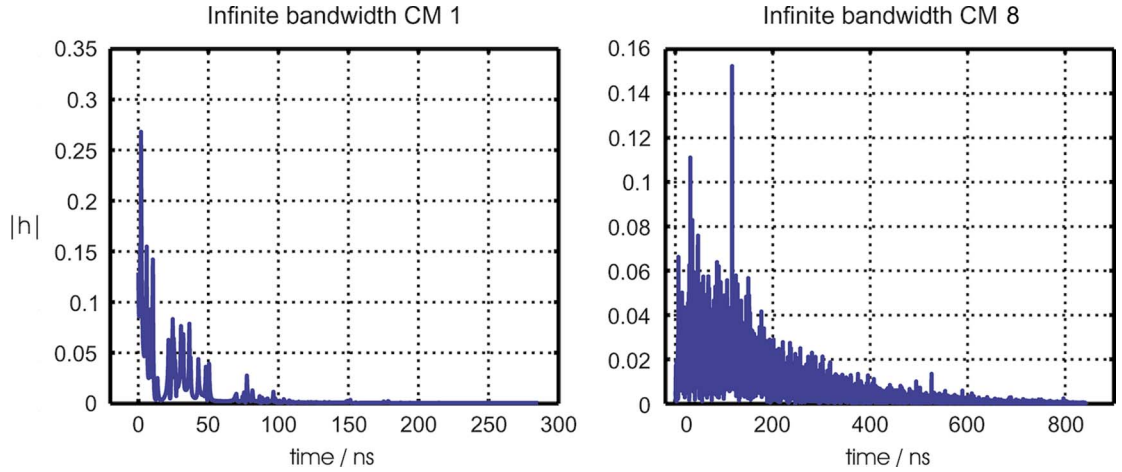

Fig. 7. *(Left) Multicluster SV impulse response in residential environment and (right) single-cluster with soft onset in industrial environment.*

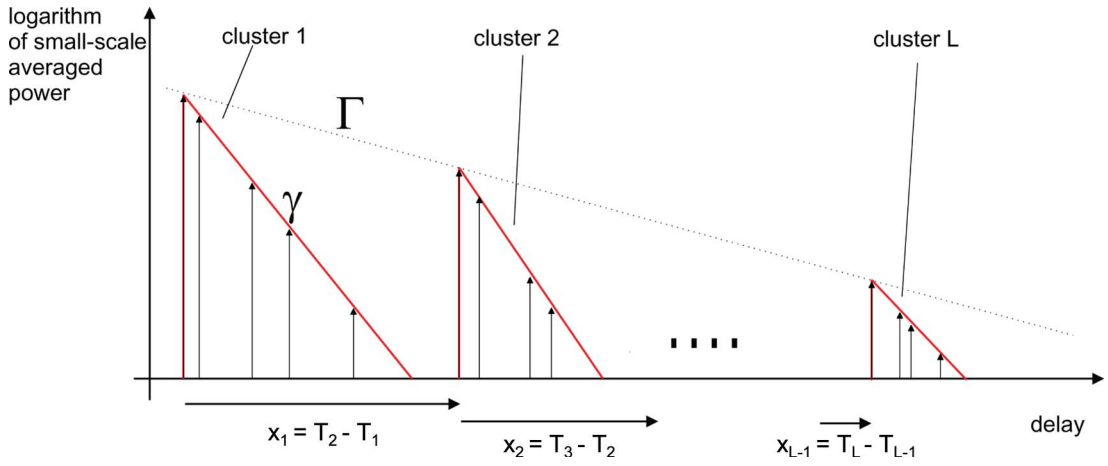

Fig. 8. *The Saleh–Valenzuela model.*

following we list some (but by no means all) interactions with modulation formats, receiver structures, etc.

As discussed in Section II-C, frequency-domain transmission techniques are mostly influenced by the shape of the PDP, i.e., how much energy arrives with how much delay. The performance is very little influenced by whether a channel is dense or sparse.

For time-domain transmission techniques, the number of resolvable MPCs is the vital quantity (see Section II-C). It is determined by the system bandwidth and the excess delay, as well as whether the channel is sparse. Clearly a sparse channel has fewer MPCs, and thus requires fewer correlators than a dense channel with the same excess delay. In practice, many receivers use simplified Rake structures: *selective* Rake (SRake) receivers, which collect the energy from the *L strongest* MPCs, and *partial* Rake (PRake) receivers, which collect the energy from the *L first* MPCs. The performance of such receivers also strongly depends on the delay dispersion characteristics. For dense channels and monotonic PDPs, PRake receivers collect most of the energy, as the MPCs with the (on average) highest energy are the ones collected by the PRake [92]. For sparse channels, PRake receivers do not perform well because they use some of the correlators to receive delay bins that do not contain MPCs. An alternative to Rake receivers is provided by time-reversal systems, where the transmit signal is predistorted according to the impulse response of the channel so that the receiver "sees" an effective impulse response that is equal to the autocorrelation function of the channel, and thus provides good concentration of the energy at the zero-lag tap [93], [94].

For noncoherent reception of time-domain transmission techniques, channel sparseness can lead to considerable performance loss. A typical noncoherent receiver takes the magnitude (or squared magnitude) of the received signal and integrates it over a time duration that is related to the delay spread. This can also be interpreted as summing up the energies in a number of *contiguous* resolvable delay bins. In a sparse channel, many of those delay bins contain only noise energy, so that the signal-to-noise ratio of the total received signal is low. A similar situation occurs in transmitted-reference systems [95]–[97].

A further complication arises in sparse UWB-REL channels. It is well known that an optimum receiver should correlate the received signal with the pulse shape corresponding to the *received* signal carried by each MPC. In narrow-band systems, this is equivalent to correlating with the pulse shape of the *transmit* pulse, giving rise to the standard "matched filter." However, for UWB-REL systems, the transmitted and received pulse shapes corresponding to a given MPC may be different. Thus, the receiver must either have a matched filter that is matched to the convolution of the transmit pulse with the function $\chi(\tau)$ (which is not feasible in practice, especially if $\chi(\tau)$ is different for each MPC) or it must use several Rake fingers for each MPC, spaced at the Nyquist sampling distance, to collect the whole energy of this MPC [98], [99]. From a practical perspective, the effect of filter mismatch is often of limited importance in UWB systems, especially if the relative BW of the system is smaller than 100% and/or the variations of the mean path loss as function of frequency are mild. It must also be noted that a Rake receiver whose correlators are spaced regularly at delays corresponding to Nyquist sampling can implement a filter that is ideally matched to the instantaneous impulse response irrespective of the underlying propagation processes. Pulse distortion compensation in time-reversal systems is discussed in [100].

For ranging, it is essential to determine the absolute delay of the *first* arriving MPC; see [101]. This task is most easily achieved if the first MPC is the strongest. Most channel models assume that this situation occurs, at least when considering the PDP. Simulations with such a model will usually result in optimistic estimates of the ranging capabilities. Other models assume a weak first component,

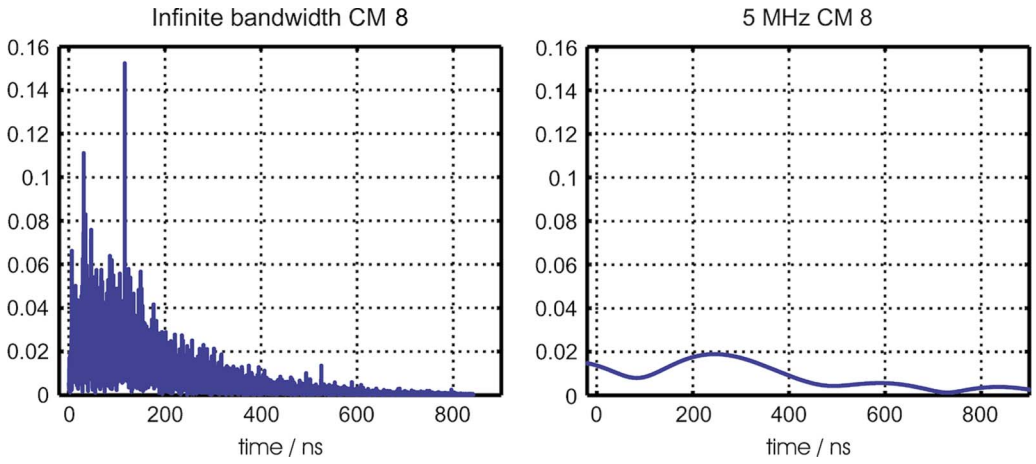

Fig. 9. ***Soft onset in industrial environment and filtered by 5 MHz BW filter.***

while the subsequent components can be stronger [51]. Note that a soft onset is more important in UWB systems than in narrow-band systems, whose filters tend to "smear out" the initial rise of the impulse response; see Fig. 9. Furthermore, the cluster structure of the impulse response can increase the difficulty of extracting the quasi-LOS component [102].

C. Angular Dispersion and Polarization

Analysis of multiple-antenna UWB systems requires the description and measurement of the angular dispersion of UWB propagation channels. It is well known from the multiple-input multiple-output literature that antenna arrays at TX and RX lead to the highest capacity when the signals at the antenna elements are decorrelated. A number of measurements of UWB spatial correlation have been reported in the literature [103]–[109]. In general, the papers indicate correlation coefficients below 0.5 for antenna spacings between 3 and 8 cm.

For a more detailed view, especially for information-theoretic considerations and the analysis of OFDM systems, it is interesting to consider the correlation behavior in the frequency domain, i.e., define a frequency-dependent correlation that is valid in bands of width Δ, centered around a frequency f. The correlation of the signals depends on one hand on the angular spread (the larger the angular spread, the lower the correlation) and on the other hand on the interelement spacing *in units of wavelength at the considered frequency* f (the larger the spacing, the lower the correlation); see also [110]. Thus in UWB-REL systems the effective interelement spacing increases with increasing frequency. At the same time, recent measurement [68] indicates that the angular spread decreases with increasing center frequency; this can be explained by the fact that some MPCs, especially those that involve diffraction, are weaker (relative to LOS) at higher frequencies. The correlation coefficient was also observed to decrease with bandwidth [111].

Measured values for angular spreads, averaged over all frequencies (or derived from time-domain measurements) have been presented in [31] and [112]–[114] for various office and residential environments. Typical angular spreads are on the order of 30–40°. Other investigations have also explored how the impulse response changes when TX and RX use directional antennas [115]. It is also noteworthy that the angular spread increases with the delay [31], [116].

Multiple-antenna systems can exploit antenna elements not only with different spatial positions but also with different polarizations [117], because fading of different polarizations is approximately uncorrelated. The capacity gain that can be achieved with such systems strongly depends on the cross-polarization discrimination of the channel. Reference [118] indicates that two orthogonal polarizations have a correlation coefficient < 0.1 but that the mean power of the co- and cross-polarized component differs by some 5 dB. A more detailed polarization model is given in [119]. The notion of polarization is particularly complex in UWB channels because the cross-polarization of both the channel and the antennas can be frequency-dependent.

D. Temporal Variations

There are two possible sources of time variance: movement of the TX or RX (or both) and/or movement of objects in the environment. If only the TX/RX moves, then the time variations are related to the angular power distribution of the MPCs and the antenna pattern [18]: if the directions of the MPCs are known, we can easily compute the effect of a movement of the TX/RX: each MPC undergoes a phase shift that is determined by the angle between the MPC and the direction of movement of TX/RX.

An even more interesting case occurs when objects are moving through the (quasi) LOS direction, thus shadowing off the most significant power contribution [120]. This leads to a time-varying attenuation; note that the attenuation by a human body can be 10 dB or more [121], though

multipath propagation decreases the effect on the total received power [122], because the MPCs provide alternative ways for the energy to get from TX to RX.

E. Special Environments

The channels discussed above are for personal-area networks (PANs), where communications occurs between devices that are typically at a distance of about 1–30 m. UWB also is promising for body-area networks (BANs), where devices located on the body of the user are talking to each other. Such arrangements are especially promising for medical applications. Extensive measurement campaigns and parameter fittings were done by Fort *et al.* [76], [77], leading to the following important insights.

i) The lognormal distribution is most suitable to describe the small-scale fading (variations of the received power at different locations within a region of stationarity) on a BAN.
ii) Strong correlation between the fading of adjacent delay bins exists.
iii) Either the lognormal distribution or the Nakagami-distribution is a suitable description for the small-scale fading due to the movement of the arms of the person on which the devices are mounted.
iv) MPCs propagating via ground reflections or wall reflections are important for the propagation between antennas on the front and back of the torso and lead to a significant increase in the delay spread.

Further investigations of BAN channels can be found in [122]–[128].

Another possible area of application lies in communications between different circuit boards in desktop computers. Using small antennas that are integrated on the circuit boards, wireless UWB links can replace the currently used cable connections, thus simplifying automated installation and integration of a card into a computer. The impulse response is dense, and results depend very little on the location of the TX and RX inside the computer casings [129], [130]. Yet another special situation of interest is UWB propagation within cars [131], [132] and ships [133].

VI. RAY-TRACING AND STATISTICAL CHANNEL MODELS

A. Ray Tracing

For system deployment, it is often necessary to know the channel behavior in a specific location. Such *site-specific* channel description requires either measurements in that location, or the solution of Maxwell's equation (or an approximation thereof) under the specific boundary conditions of the location. Ray tracing or ray launching, which use a high-frequency approximation to Maxwell's equations, are well-established tools for site-specific channel modeling in the context of cellular networks. In other words, ray tracing emits rays (representing homogeneous plane waves) from the transmitter and computes the interaction of those rays with the environment. Standard, narrow-band ray tracing assumes that each interaction leads to an attenuation as well as a change of direction of a ray (e.g., when it is reflected on a wall); the path of the ray also determines its runtime and thus its delay. The characteristics (delay, runtime, direction) of all the rays determines the impulse response.

UWB-REL channels pose additional challenges for ray tracing due to the frequency selectivity of the propagation processes (reflection, diffraction, etc.). One possible solution performs traditional ray tracing at different frequencies and then combines the results [134]. An alternative computes the distortion functions $\chi(t)$ of the different rays (which depends on the interaction processes they go through) and adds up the contributions from the different rays [135]–[137]. In either case a theoretical and/or experimental understanding of the frequency selectivity of propagation processes is essential [11], [23], [138]–[148]. When comparing ray tracing to measurements, we find that most ray-tracing results underestimate the number of MPCs. Consequently, Rake receivers designed on the basis of ray tracing results tend to have a lower number of correlators. To enhance the simulation accuracy for smaller objects, there are proposals to include full wave simulation to describe scattering from small objects, which leads to hybrid simulation procedures [149], [150].

Another possible approach lies in combining *deterministic* components that are derived from ray tracing with a Rayleigh-distributed "clutter" that describes the contributions that stem from diffuse scattering and other propagation paths that are not covered by the ray tracing [46], [66], [151].

B. Standardized Statistical Models

For system design, especially in the context of system standardization, *site-independent* channel models are required. Such models serve as a reference that is used for the simulation of different system proposals. Two models are in widespread use: the IEEE 802.15.3a model and the IEEE 802.15.4a model.

The 802.15.3a model was developed in 2003 by a standardization group for UWB communications systems in order to compare standardization proposals for high-data-rate wireless PANs [152], [153]. Due to this purpose, the considered environments were office and residential indoor scenarios with a distance between TX and RX of less than 10 m. The model distinguishes between four radio environments: LOS with a distance between TX and RX of 0–4 m (CM1), NLOS for a distance 0–4 m (CM2), NLOS for a distance 4–10 m (CM3), and a "heavy multipath" environment (CM4). The model is a "classical" SV model, with parameterization derived from measurements [73], [154].

The IEEE 802.15.4a was a group that developed a standard for UWB-based low-data-rate communications

with ranging capability; see [155]. For the system selection, it developed a UWB channel model [67] that is valid over larger distances than the 802.15.3a model. The model is parameterized for LOS as well as non-LOS situations in residential indoor, office indoor, industrial, outdoor, and farm environments. Some of the environments (industrial non-LOS, office non-LOS) use a dense channel model with a "soft onset" of the power delay profile, while others use a generalized SV model. In addition 802.15.4a contains a model for BANs based on [76] and [77], as well as a model for office environments in the 300–1000 MHz range based on [30] and also [156].

The 802.15.4a model is more general and based on more measurements than the earlier 3a model. It is noteworthy that both the 15.3a and the 15.4a channel models are suitable for simulations of UWB systems with arbitrary data rates.[16]

VII. SUMMARY AND CONCLUSION

This paper presented an overview of UWB propagation channels, stressing the fundamental differences from conventional (narrow-band and wide-band) propagation channels and discussing the impact on system design. We found that we have to distinguish between UWB channels with large absolute bandwidth and UWB channels with large relative bandwidth, as the behavior and peculiarities are different for those cases. For UWB-REL channels, all fundamental propagation processes, like reflection, diffraction, become frequency dependent. Consequently:

- the channel impulse response is a sum of delayed, attenuated, *and distorted* MPCs;
- the system cannot be described in the framework of WSSUS (wide-sense-stationary uncorrelated scattering) systems [25];
- matched filters that are matched to the transmit signal might not be optimum;
- for OFDM and multiband signals, the link capacity is the summation of the capacities of the different subcarriers or subbands, which in turn decrease with increasing frequency;
- also channel parameters like delay spread, angular spread, etc., can depend on the frequency.

For UWB-ABS channels, several effects can occur (depending on the environment).

- The channel impulse response can become sparse, i.e., not every resolvable delay bin contains significant MPCs.
- For such a sparse impulse response, a relatively small number of Rake fingers can collect most of the received energy. Requirements for OFDM systems, on the other hand, are hardly influenced by sparseness of impulse response.
- The fading statistics of the absolute amplitudes usually are not Rayleigh; in other words, the fading depth is smaller than in narrow-band systems.
- The PDP can show a "soft onset," which makes ranging more difficult.

We also discussed that the measurement and subsequent evaluation of UWB-REL channels poses some unique challenges, several of which are not completely solved yet. Last, but not least, it must be emphasized that our current picture of UWB channels is based on only a rather small number measurement campaigns, at least compared to cellular and WLAN systems. Thus, parameter settings that are seen as "typical" today might actually only be true for the environment in which the one existing measurement campaign was done. More experimental work will be needed in the future. ■

[16]It is a common misconception that the 15.3a model is particularly suited for the simulation of high-data-rate systems while the 15.4a model is for low-rate systems. However, a channel model is *not* dependent on data rate, modulation format, etc., of the system using it.

Acknowledgment

The author would like to express his deep gratitude to Prof. L. Greenstein, whose many detailed and constructive comments greatly improved this paper. The author thanks J. Karedal, T. Santos, and Dr. Z. Sahinoglu for critical reading of the manuscript; Dr. P. Orlik for creating the filtered impulse responses of Figs. 6, 7, and 9; and T. Santos for creating Figs. 2 and 5. Many useful discussions with Prof. M. Win, Dr. D. Cassioli, Prof. R. Qiu, Prof. R. Scholtz, Dr. S. Ghassemzadeh, Dr. J. Foerster, Dr. M. Pendergrass, Prof. F. Tufvesson, Dr. C.-C. Chong, Dr. K. Balakrishnan, Dr. S. Emami, Dr. A. Fort, Dr. J. Kunisch, U. Schuster, and Dr. J. Zhang impacted the author's view of UWB channels. The comments of the anonymous reviewers greatly helped to improve the clarity of this paper.

REFERENCES

[1] R. A. Scholtz, "Multiple access with time-hopping impulse modulation," in *Proc. IEEE Military Commun. Conf. (MILCOM)*, Boston, MA, Oct. 1993, vol. 2, pp. 447–450.

[2] M. Z. Win and R. A. Scholtz, "Impulse radio: How it works," *IEEE Commun. Lett.*, vol. 2, pp. 36–38, Feb. 1998.

[3] M. Z. Win and R. A. Scholtz, "Ultra-wide bandwidth time-hopping spread-spectrum impulse radio for wireless multiple-access communications," *IEEE Trans. Commun.*, vol. 48, pp. 679–691, Apr. 2000.

[4] "First report and order 02-48," Federal Communications Comission, 2002.

[5] "Uwb: High rate ultra wideband PHY and MAC standard," Eur. Comput. Manuf. Assoc., 2005, Tech. Rep. [Online]. Available: www.ecma-international.org

[6] S. Gezici, H. Kobayashi, H. V. Poor, and A. F. Molisch, "Performance evaluation of impulse radio UWB systems with pulse-based polarity randomization," *IEEE Trans. Signal Process.*, vol. 53, pp. 2537–2549, Jul. 2005.

[7] M. G. diBenedetto, T. Kaiser, A. F. Molisch, I. Oppermann, C. Politano, and D. Porcino, Eds., *UWB Communications Systems: A Comprehensive Overview*. Cairo, Egypt: Hindawi, 2006.

[8] M. Ghavami, L. B. Michael, and R. Kohno, *Ultra Wideband Signals and Systems in Communication Engineering*. New York: Wiley, 2004.

[9] L. Yang and G. B. Giannakis, "Ultra-wideband communications—An idea whose time has come," *IEEE Signal Process. Mag.*, vol. 21, pp. 26–54, Nov. 2004.

[10] R. C. Qiu, H. Liu, and X. Shen, "Ultra-wideband for multiple access communications," *IEEE Commun. Mag.*, vol. 43, pp. 80–87, Feb. 2005.

[11] R. C. Qiu, "Propagation effects," in *UWB Communications Systems: A Comprehensive Overview*, M. G. Di Benedetto *et al.*, Eds. Cairo, Egypt: Hindawi, 2006.

[12] R. C. Qiu, "A study of the ultra-wideband wireless propagation channel and optimum UWB receiver design," *IEEE J. Sel. Areas. Comm.*, vol. 20, pp. 1628–1637, Dec. 2002.

[13] D. Cassioli, M. Z. Win, and A. F. Molisch, "A statistical model for the UWB indoor channel," in *Proc. 53rd IEEE Veh. Technol. Conf.*, May 2001, vol. 2, pp. 1159–1163.

[14] B. Allen, M. Dohler, E. E. Okon, W. Q. Malik, A. K. Brown, and D. J. Edwards, Eds., *Ultra-Wideband Antennas and Propagation for Communications, Radar and Imaging*. New York: Wiley, 2006.

[15] A. F. Molisch, "Ultrawideband propagation channels—Theory, measurement, and modeling," *IEEE Trans. Veh. Technol.*, vol. 54, pp. 1528–1545, Sep. 2005.

[16] A. F. Molisch, "Ultrawideband propagation channels and their impact on system design," in *Proc. IEEE Conf. Meas., Antennas, Channels, EMC (MAPE)*, 2007.

[17] J. Ahmadi-Shokouh and R. Qiu, "Ultra-wideband (UWB) communications—A tutorial review," submitted for publication.

[18] A. F. Molisch, *Wireless Communications*. New York: Wiley, 2005.

[19] A. F. Molisch and F. Tufvesson, "Multipath propagation models for broadband wireless systems," in *CRC Handbook of Signal Processing for Wireless Commmunications*, M. Ibnkahla, Ed. Boca Raton, FL: CRC Press, 2004.

[20] V. DegliEsposti, D. Guiducci, A. deMarsi, P. Azzi, and F. Fuschini, "An advanced field prediction model including diffuse scattering," *IEEE Trans. Antennas Propag.*, vol. 52, pp. 1717–1728, 2004.

[21] A. Richter and R. S. Thomae, "Joint maximum likelihood estimation of specular paths and distributed diffuse scattering," in *Proc. Veh. Technol. Conf. 2005 Spring*, 2005, pp. 11–15.

[22] T. Fugen, J. Maurer, T. Kayser, and W. Wiesbeck, "Verification of 3d ray-tracing with non-directional and directional measurements in urban macrocellular environments," in *Proc. IEEE 63rd Veh. Technol. Conf.*, 2006, pp. 2661–2665.

[23] R.-R. Lao, J.-H. Tarng, and C. Hsiao, "Transmission coefficients measurement of building materials for UWB systems in 3–10 GHz," in *Proc. IEEE Veh. Technol. Conf. Spring*, 2003, pp. 11–14.

[24] T. Santos, J. Karedal, P. Almers, F. Tufvesson, and A. F. Molisch, "Scatterer detection by successive cancellation for UWB—Method and experimental verification," in *Proc. IEEE VTC Spring 2008*, 2008.

[25] P. A. Bello, "Characterization of randomly time-variant linear channels," *IEEE Trans. Commun.*, vol. 11, pp. 360–393, 1963.

[26] P. A. Bello, "Evaluation of mobile ultra wideband modems in dense multipath—Part 1: Channel model," *IEEE Trans. Wireless Commun.*, vol. 6, pp. 4145–4153, 2007.

[27] M. Z. Win and G. Chrisikos, *Impact of Spreading Bandwidth and Selection Diversity Order on Rake Reception*. Englewood Cliffs, NJ: Prentice-Hall, 2001, ch. 29.

[28] M. Z. Win and R. A. Scholtz, "On the energy capture of ultra-wide bandwidth signals in dense multipath environments," *IEEE Commun. Lett.*, vol. 2, pp. 245–247, Sep. 1998.

[29] J. Keignart and N. Daniele, "Subnanosecond UWB channel sounding in frequency and temporal domain," in *Proc. UWBST 2002*, 2002, pp. 25–30.

[30] D. Cassioli, M. Z. Win, and A. F. Molisch, "The ultra-wide bandwidth indoor channel: From statistical model to simulations," *IEEE J. Sel. Areas Commun.*, pp. 1247–1257, 2002.

[31] R. J.-M. Cramer, R. A. Scholtz, and M. Z. Win, "Evaluation of an ultra-wide-band propagation channel," *IEEE Trans. Antennas Propag.*, vol. 50, pp. 561–570, May 2002.

[32] D. Cassioli and A. Durantini, "A time domain propagation model of the UWB indoor channel in the FCC-compliant band 3.6–6 GHz based on pn-sequence channel measurements," in *Proc. VTC 04 Spring*, 2004, pp. 213–217.

[33] U. G. Schuster and H. Boelcskei, "Ultrawideband channel modeling on the basis of information-theoretic criteria," *IEEE Trans. Wireless Commun.*, vol. 6, pp. 2464–2475, 2007.

[34] G. Matz, A. F. Molisch, F. Hlawatsch, M. Steinbauer, and I. Gaspard, "On the systematic measurement errors of correlative mobile radio channel sounders," *IEEE Trans. Commun.*, vol. 50, pp. 808–821, 2002.

[35] A. Bayram, A. M. Attiya, A. Safaai-Jazi, and S. M. Riad, "Frequency-domain measurement of indoor uwb propagation," in *Proc. IEEE Antennas Propag. Symp.*

[36] W. Q. Malik, D. J. Edwards, and C. J. Stevens, "Angular-spectral antenna effects in ultra wideband communications links," *Proc. Inst. Elect. Eng. Commun.*, vol. 153, pp. 99–106, 2006.

[37] J. G. Maloney, G. S. Smith, and W. R. Scott, "Accurate computation of the radiation from simple antennas using the finite-difference time-domain method," *IEEE Trans. Antennas Propag.*, vol. 38, pp. 1059–1068, 1990.

[38] J. Kunisch, "Measurement procedures," in *UWB Communications Systems—A Comprehensive Overview*, M. G. Di Benedetto *et al.*, Eds. Cairo, Egypt: Hindawi, 2006.

[39] M. Sachs, P. Kmec, P. Peyerl, A. Rauschenbach, R. Thomä, and R. Zetik, "A novel ultra-wideband real-time MIMO channel sounder architecture," in *Proc. URSI General Assembly*, 2005.

[40] H. Krim and M. Viberg, "Two decades of array signal processing research," *IEEE Signal Process. Mag.*, pp. 67–93, 1996.

[41] B. H. Fleury, M. Tschudin, R. Heddergott, D. Dahlhaus, and I. K. Pedersen, "Channel parameter estimation in mobile radio environments using the sage algorithm," *IEEE J. Sel. Areas Commun.*, pp. 434–450, 1999.

[42] K. Haneda and J. I. Takada, "An application of SAGE algorithm for UWB propagation channel estimation," in *Proc. IEEE UWBST 03*, 2003, pp. 483–487.

[43] K. Haneda, J. I. Takada, and K. Kobayashi, "Experimental evaluation of a SAGE algorithm for ultra wideband channel sounding in an anechoic chamber," in *Proc. IEEE UWBST 04*, 2004, pp. 66–70.

[44] K. Haneda, J. Takada, and T. Kobayashi, "A parametric uwb propagation channel estimation and its performance validation in an anechoic chamber," *IEEE Trans. Microwave Theory Tech.*, vol. 54, pp. 1802–1811, 2006.

[45] W. Q. Malik, C. J. Stevens, and D. J. Edwards, "Synthetic aperture analysis of multipath propagation in the ultra-wideband communications channel," in *Proc. IEEE Workshop Signal Process. Adv. Wireless Commun.*, 2005.

[46] J. Kunisch and J. Pamp, *An ultra-wideband space-variant multipath indoor radio channel model, Proc. IEEE UWBST*, 2003, pp. 290–294.

[47] G. T. F. Abreu, "Performance of parameter estimation from UWB-IR signals with an array of orthonormal correlators," in *IEEE Int. Conf. Ultra-Wideband 2005*, 2005, pp. 542–547.

[48] R. D. Balakrishnan and H. M. Kwon, "Estimation of channel parameters using iterative least squares approach for W-CDMA and UWB systems," in *Proc. Asilomar Conf. Signals, Syst. Comput.*, 2003, pp. 1254–1258.

[49] S. M. Yano, "Investigating the ultra-wideband indoor wireless channel," in *Proc. 55th IEEE Veh. Technol. Conf. Spring*, 2002, vol. 3, pp. 1200–1204.

[50] J. Keignart, J.-B. Pierrot, N. Daniele, A. Alvarez, M. Lobeira, J. L. Garcia, G. Valera, and R. P. Torres, "U.C.A.N. report on UWB basic transmission loss," Tech. Rep. IST-2001-32710-U.C.A.N., Mar. 2003.

[51] J. Karedal, S. Wyne, P. Almers, F. Tufvesson, and A. F. Molisch, "A measurement-based statistical model for ultra-wideband industrial channels," *IEEE Trans. Wireless Commun.*, vol. 6, pp. 3028–3037, 2007.

[52] D. Cassioli, W. Ciccognani, and A. Durantini, "D3.1—UWB channel model report," Tech. Rep. IST-2001-35189-ULTRAWAVES, Nov. 2003.

[53] A. Durantini, W. Ciccognani, and D. Cassioli, "UWB propagation measurements by PN-sequence channel sounding," in *Proc. IEEE Int. Conf. Commun.*, Paris, France, Jun. 2004.

[54] B. Kannan *et al.*, "UWB channel characterization in office environments," Tech. Rep. Doc. IEEE 802.15-04-0439-00-004a, 2004.

[55] C. C. Chong, Y. Kim, and S. S. Lee, "A modified S-V clustering channel model for the UWB indoor residential environment," in *Proc. IEEE VTC Spring 05*, 2005.

[56] S. Ghassemzadeh, L. J. Greenstein, A. Kavcic, T. Sveinsson, and V. Tarokh, "An empirical indoor path loss model for ultra-wideband channels," *J. Commun. Netw. [Special Issue on Ultra-Wideband (UWB) Communications]*, vol. 5, pp. 303–308, 2003.

[57] S. S. Ghassemzadeh, R. Jana, C. W. Rice, W. Turin, and V. Tarokh, "Measurement and modeling of an ultra-wide bandwidth indoor channel," *IEEE Trans. Commun.*, vol. 52, pp. 1786–1796, Oct. 2004.

[58] V. Erceg *et al.*, "An empirically based path loss model for wireless channels in suburban environments," *IEEE. J. Sel. Areas Commun.*, vol. 17, pp. 1205–1211, 1999.

[59] B. Kannan *et al.*, "UWB channel characterization in outdoor environments," Tech. Rep. Doc. IEEE 802.15-04-0440-00-004a, 2004.

[60] S. S. Ghassemzadeh, L. J. Greenstein, T. Sveinsson, A. Kavcic, and V. Tarokh, "UWB indoor path loss model for residential and commercial environments," in *IEEE VTC 2003 Fall*, pp. 3115–3119.

[61] G. Kadel and R. W. Lorenz, "Impact of the radio channel on the performance of digital mobile communication systems," in *Proc. 6th IEEE Int. Symp. Personal, Indoor Mobile Radio Commun. (PIMRC '95)*, 1995, pp. 419–423.

[62] J.-P. Rossi, "Influence of measurement conditions on the evaluation of some radio channel parameters," *IEEE Trans. Veh. Technol.*, vol. VT-48, pp. 1304–1316, Jul. 1999.

[63] B. M. Donlan, D. R. McKinstry, and R. M. Buehrer, "The UWB indoor channel: Large and small scale modeling," *IEEE Trans. Wireless Commun.*, vol. 5, pp. 2863–2873, 2006.

[64] R. C. Qiu and I.-T. Lu, "Wideband wireless multipath channel modeling with path frequency dependence," in *Proc. IEEE Intl. Conf. Commun.*, Dallas, TX, Jun. 1996, pp. 277–281.

[65] R. C. Qiu and I.-T. Lu, "Multipath resolving with frequency dependence for broadband wireless channel modeling," *IEEE Trans. Veh. Technol.*, vol. 48, pp. 273–285, Jan. 1999.

[66] J. Kunisch and J. Pamp, "Measurement results and modeling aspects for the UWB radio channel," in *Proc. IEEE UWBST*, 2002, pp. 19–23.

[67] A. F. Molisch, K. Balakrishnan, C. C. Chong, D. Cassioli, S. Emami, A. Fort, J. Karedal, J. Kunisch, H. Schantz, K. Siwiak, and M. Z. Win, "A comprehensive model for ultrawideband propagation channels," *IEEE Trans. Antennas Propag.*, pp. 3151–3166, 2006.

[68] W. Q. Malik, D. J. Edwards, and C. J. Stevens, "Frequency dependence of fading statistics for ultrawideband systems," *IEEE Trans. Wireless Commun.*, vol. 6, pp. 800–804, 2007.

[69] T. S. Chu and L. J. Greenstein, "A quantification of link budget differences between the cellular and pcs bands," *IEEE Trans. Veh. Technol.*, vol. 48, pp. 60–65, 1999.

[70] D. Cassioli, A. Durantini, and W. Ciccognani, "The role of path loss on the selection of the operating bands of UWB systems," in *Proc. IEEE Int. Symp. Personal, Indoor Mobile Radio Commun.*, Barcelona, Spain, Sep. 2004.

[71] A. Alvarez, G. Valera, M. Lobeira, R. Torres, and J. L. Garcia, "New channel impulse response model for UWB indoor system simulations," in *Proc. VTC 2003 Spring*, 2003, pp. 1–5.

[72] V. Hovinen, M. Hämäläinen, and T. Pätsi, "Ultra wideband indoor radio channel models: Preliminary results," in *Proc. IEEE UWBST*, 2002, pp. 75–79.

[73] J. R. Foerster and Q. Li, "UWB channel modeling contribution from Intel," Tech. Rep. P802.15 02/279SG3a, 2002, IEEE P802.15 SG3a contribution.

[74] H. Zhang, T. Udagawa, T. Arita, and M. Nakagawa, "A statistical model for the small-scale multipath fading characteristics of ultra-wideband indoor channel," in *Proc. IEEE UWBST*, 2002, pp. 81–85.

[75] S. Z. H. Lüdiger, B. Kull, and A. Finger, "An ultra-wideband indoor NLOS radio channel amplitude probability density distribution," in *Proc. Int. Symp. Spread-Spectrum Tech. Applicat.*, Prague, Czech Republic, Oct. 2002, pp. 68–72.

[76] A. Fort, P. P. Desset, C. Wambacq, and L. Van Biesen, "An ultra-wideband body area propagation channel model-from statistics to implementation," *IEEE Trans. Microwave Theory Tech.*, vol. 54, pp. 1820–1826, 2006.

[77] A. Fort, J. Ryckaert, C. Desset, P. DeDoncker, P. Wambacq, and L. VanBiesen, "Ultra-wideband channel model for communication around the human body," *IEEE J. Sel. Areas Commun.*, vol. 24, pp. 927–933, 2006.

[78] G. L. Turin, F. D. Clapp, T. L. Johnston, S. B. Fine, and D. Lavry, "A statistical model of urban multipath propagation," *IEEE Trans. Veh. Technol.*, vol. VT-21, pp. 1–9, Feb. 1972.

[79] A. F. Molisch, H. Asplund, R. Heddergott, M. Steinbauer, and T. Zwick, "The COST259 directional channel model—I. Overview and methodology," *IEEE Trans. Wireless Commun.*, vol. 5, pp. 3421–3433, 2006.

[80] N. Czink, P. Cera, J. Salo, E. Bonek, J.-P. Nuutinen, and J. Ylitalo, "Improving clustering performance by using the multi-path component distance," *Electron. Lett.*, vol. 42, pp. 44–45, 2006.

[81] A. A. M. Saleh and R. A. Valenzuela, "A statistical model for indoor multipath propagation," *IEEE J. Sel. Areas Commun.*, vol. SAC-5, pp. 128–137, Feb. 1987.

[82] A. F. Molisch *et al.*, "IEEE 802.15.4a channel model—Final report," Tech. Rep. Doc. IEEE 802.15-04-0662-02-004a, 2005.

[83] C. C. Chong and S. K. Yong, "A generic statistical-based uwb channel model for high-rise apartments," *IEEE Trans. Antennas Propag.*, pp. 2389–2399, 2005.

[84] A. Hugine, H. I. Volos, J. Gaeddert, and R. M. Buehrer, "Measurement and characterization of the near-ground indoor ultra wideband channel," in *Proc. Wireless Commun. Netw. Conf.*, 2006.

[85] M. diRenzo, F. Graziosi, R. Minutolo, M. Montanari, and F. Santucci, "The ultra-wide bandwidth outdoor channel: From measurement campaign to statistical modelling," *Mobile Netw. Applicat.*, vol. 11, pp. 452–467, 2006.

[86] C. W. Kim, X. Sun, L. C. Chiam, B. Kannan, F. P. S. Chin, and H. K. Garg, "Characterization of ultra-wideband channels for outdoor office environment," in *Wireless Commun. Netw. Conf.*, 2005, pp. 950–955.

[87] W. J. Chang and J.-H. Tarng, "Effects of bandwidth on observable multipath clustering in outdoor/indoor environments for broadband and ultrawideband wireless systems," *IEEE Trans. Veh. Technol.*, vol. 56, pp. 1913–1923, 2007.

[88] A. S. Y. Poon and M. Ho, "Indoor multiple-antenna channel charaterization from 2 to 8 GHz," in *Proc. IEEE Int. Conf. Commun.*, May 2003, pp. 3519–3523.

[89] S. Venkatesh, J. Ibrahim, and R. M. Buehrer, "A new 2-cluster model for indoor UWB channel measurements," in *Proc. IEEE Antennas Propag. Symp.*, 2004, pp. 946–949.

[90] S. S. Ghassemzadeh, L. J. Greenstein, T. Sveinsson, and V. Tarokh, "UWB delay profile models for residential and commercial indoor environments?" *IEEE Trans. Veh. Technol.*, pp. 1235–1244, 2005.

[91] L. J. Greenstein, S. S . Ghassemzadeh, S. C. Hong, and V. Tarokh, "Comparison study of UWB indoor channel models," *IEEE Trans. Wireless Commun.*, vol. 6, pp. 128–135, 2007.

[92] D. Cassioli, M. Z. Win, F. Vatalaro, and A. F. Molisch, "Low-complexity rake receivers in ultra-wideband channels," *IEEE Trans. Wireless Commun.*, vol. 6, pp. 1265–1275, 2007.

[93] R. C. Qiu, "A theory of time-reversed impulse multiple-input multiple-output (MIMO) for ultra-wideband (UWB) communications," in *IEEE Int. Conf. Ultra-Wideband (ICUWB06)*, 2006.

[94] N. Guo, R. C. Qiu, and B. M. Sadler, "Reduced-complexity time reversal enhanced autocorrelation receivers considering experiment-based uwb channels," *IEEE Trans. Wireless Commun.*, vol. 6, Dec. 2007.

[95] J. D. Choi and W. E. Stark, "Performance of ultra-wideband communications with suboptimal receivers in multipath channels," *IEEE J. Sel. Areas Commun.*, vol. 20, pp. 1754–1766, Dec. 2002.

[96] T. Q. S. Quek and M. Z. Win, "Analysis of UWB transmitted reference communication systems in dense multipath channels," *IEEE J. Sel. Areas Commun.*, vol. 23, pp. 1863–1874, Sep. 2005.

[97] F. Tufvesson, S. Gezici, and A. F. Molisch, "Ultra-wideband communications using hybrid matched filter correlation receivers," *IEEE Trans. Wireless Commun.*, vol. 5, pp. 3119–3129, 2006.

[98] R. C. Qiu, "A generalized time domain multipath channel and its application in ultra-wideband (UWB) wireless optimal receiver design: Wave-based system ananlysis," *IEEE Trans. Wireless Commun.*, vol. 4, pp. 2312–2324, 2004.

[99] R. C. Qiu, "A generalized time domain multipath channel and its application in ultrawideband UWB wireless optimal receiver design: System performance analysis," in *Proc. IEEE Wireless Comm. Network. Conf.*, 2004, pp. 901–907.

[100] R. C. Qiu, J. Q. Zhang, and N. Guo, "Detection of physics-based ultra-wideband signals using generalized rake and multi-user detection (MUD)," *IEEE J. Sel. Areas Commun.*, vol. 24, pp. 724–730, 2006.

[101] S. Gezici and H. V. Poor, "Position estimation via ultra-wideband signals," *Proc. IEEE*, vol. 97, no. 2, Feb. 2009.

[102] I. Guvenc, Z. Sahinoglu, A. F. Molisch, and P. Orlik, "Non-coherent TOA estimation in ir-uwb systems with different signal waveforms," in *Proc. IEEE UWBNet Conf.*, 2005, pp. 245–251.

[103] H. Agus, J. Nielsen, and R. J. Davies, "Correlation analysis for indoor UWB channel," in *Proc. Wireless 2005*, 2005.

[104] C. Prettie, D. Cheung, L. Rusch, and M. Ho, "Spatial correlation of UWB signals in a home environment," in *Proc. IEEE UWBST*, 2002, pp. 65–70.

[105] J. Liu, B. Allen, W. Q. Malik, and D. J. Edwards, "A measurement based spatial correlation analysis for MBOFDM ultra wideband transmissions," in *Proc. Loughborough Ant. Propagat. Conf.*, 2005.

[106] M. Chamchoy, S. Promwong, P. Tangtisanon, and J. Takada, "Spatial correlation properties of multiantenna uwb systems for in-home scenarios," in *Proc. IEEE Int. Symp. Commun. Inf. Technol. '04*, 2004, pp. 1029–1032.

[107] V. P. Tran and A. Sibille, "UWB spatial multiplexing by multiple antennas and rake decorrelation," in *Proc. 2nd Int. Symp. Wireless Commun. Syst.*, 2005, pp. 272–276.

[108] J. Keignart, C. Abou-Rjeily, C. Delaveaud, and N. Daniele, "Uwb simo channel measurements and simulations," *IEEE Trans. Microwave Theory Tech.*, vol. 54, pp. 1812–1819, 2006.

[109] X. Hong, C. X. Wang, B. Allen, and W. Q. Malik, "Correlation-based double-directional stochastic channel model for multiple-antenna ultra-wideband systems," *IET Microw. Antennas Propag.*, vol. 1, pp. 1182–1191, 2007.

[110] T. Kaiser, "UWB-MIMO systems," *Proc. IEEE*, vol. 97, no. 2, Feb. 2009.

[111] W. Q. Malik, "Spatial correlation in ultrawideband channels," *IEEE Trans. Wireless Commun.*, vol. 7, pp. 604–610, 2008.

[112] J. M. Cramer, R. A. Scholtz, and M. Z. Win, "Spatiotemporal diversity in ultra-wideband radio," in *Proc. IEEE Wireless Commun. Netw. Conf.*, 1999.

[113] J. Takada, F. Ohkubo, K. Haneda, and T. Kobayashi, "Ultra wideband double-directional channel measurements in an office environment," in *Proc. IEEE Int. Conf. Ultra-Wideband*, 2005.

[114] K. Haneda, J. I. Takada, and T. Kobayashi, "Double directional ultra wideband channel characteriation in a line-of-sight home environment," *IEICE Trans. Fundamentals*, vol. E88-A, pp. 2264–2271, 2005.

[115] J. A. Dabin, A. M. Haimovich, and H. Grebel, "A statistical ultra-wideband indoor channel model and the effects of antenna directivity on path loss and multipath propagation," *IEEE J. Sel. Areas Commun.*, vol. 24, pp. 752–758, 2006.

[116] Q. Li and W. S. Wong, "Measurement and analysis of the indoor UWB channel," in *Proc. IEEE VTC Spring*, 2003.

[117] S. Chang and R. A. Scholtz, *Polarization measurements in a UWB multipath channel*, MILCOM, 2004, pp. 192–196.

[118] W. Q. Malik, M. C. Mtumbuka, D. J. Edwards, and C. J. Stevens, "Increasing mimo capacity in ultra-wideband communications through orthogonal polarizations," in *Proc. 6th Workshop Signal Process. Adv. Wireless Commun.*, 2005, pp. 575–579.

[119] W. Q. Malik, "Polarimetric characterization of ultrawideband propagation channels," *IEEE Trans. Antennas Propag.*, vol. 56, pp. 532–539, 2008.

[120] P. Pagani and P. Pajusco, "Experimental assessment of the uwb channel variability in a dynamic indoor environment," in *Proc. IEEE PIMRC 2004*, 2004, pp. 2973–2977.

[121] Z. Irahhauten, J. Dacuna, G. J. M. Janssen, and H. Nikookar, "UWB channel measurements and results for wireless personal area networks applications," in *Proc. Eur. Conf. Wireless Technol. 2005*, 2005, pp. 189–192.

[122] T. B. Welch, R. L. Musselman, B. A. Emessiene, P. D. Gift, D. K. Choudhury, D. N. Cassadine, and S. M. Yano, "The effects of the human body on UWB signal propagation in an indoor environment," *IEEE J. Sel. Areas Commun.*, vol. 20, pp. 1778–1782, 2002.

[123] I. Kovacs, G. Pedersen, P. Eggers, and K. Olesen, "Ultra wideband radio propagation in body area network scenarios," in *Proc. IEEE ISSSTA 04*, 2004, pp. 102–106.

[124] T. Zasowski, F. Althaus, M. Stager, A. Wittneben, and G. Troster, "UWB for noninvasive wireless body area networks: Channel measurements and results," in *Proc. IEEE UWBST 03*, 2003, pp. 285–289.

[125] Y. P. Zhang, B. Li, and C. Qi, "Characterization of on-human-body UWB radio propagation channel," *Microw. Opt. Technol. Lett.*, vol. 49, pp. 1365–1371, 2007.

[126] A. Alomainy, Y. Hao, X. Hu, C. G. Parini, and P. S. Hall, "UWB on-body radio propagation and system modelling for wireless body-centric networks," *Proc. Inst. Elect. Eng. Commun.*, vol. 153, pp. 107–114, 2006.

[127] T. Zasowski, G. Meyer, F. Althaus, and A. Wittneben, "UWB signal propagation at the human head," *IEEE Trans. Microwave Theory Tech.*, vol. 54, pp. 1836–1845, 2006.

[128] A. A. Goulianos and S. Stavrou, "UWB path arrival times in body area networks," *IEEE Antennas Wireless Propag. Lett.*, vol. 6, pp. 223–226, 2007.

[129] J. Karedal, A. P. Singh, F. Tufvesson, and A. F. Molisch, "Characterization of a computer board-to-board ultra-wideband channel," *IEEE Commun. Lett.*, vol. 11, pp. 468–470, 2007.

[130] Z. M. Chen and Y. P. Zhang, "Inter-chip wireless communication channel: Measurement, characterization, and modeling," *IEEE Trans. Antennas Propag.*, vol. 55, pp. 978–986, 2007.

[131] P. C. Richardson, W. Xiang, and W. S. Stark, "Modeling of ultra-wideband channels within vehicles," *IEEE J. Sel. Areas Commun.*, pp. 906–912, 2006.

[132] R. C. Qiu, C. Zhou, J. Q. Zhang, and N. Guo, "Channel reciprocity and time-reversed propagation for ultra-wideband communications," in *Proc. IEEE AP-S Int. Symp. Antennas Propag.*, 2007.

[133] R. C. Qiu, B. Sadler, and Z. Hu, "Time reversed transmission with chirp signaling for UWB communications and its application in confined metal environments," in *Proc. IEEE ICUWB07*, 2007.

[134] H. Sugahara, Y. Watanabe, T. Ono, K. Okanoue, and S. Yarnazaki, "Development and experimental evaluations of 'RS-2000'—A propagation simulator for UWB systems," in *Proc. IEEE UWBST 04*, 2004, pp. 76–80.

[135] B. Uguen, E. Plouhinec, Y. Lostanlen, and G. Chassay, "A deterministic ultra wideband channel modeling," in *Proc. IEEE UWBST*, 2002, pp. 1–5.

[136] A. M. Attiya and A. Safaai-Jazi, "Simulation of ultra-wideband indoor propagation," *Microw. Opt. Technol. Lett.*, vol. 42, pp. 103–107, 2004.

[137] G. A. Schiavone, P. Vahid, R. Palaniappan, J. Trace, and T. Dere, "Analysis of ultra-wide band signal propagation in an indoor environment," *Microw. Opt. Technol. Lett.*, vol. 36, pp. 13–15, 2003.

[138] K. Heidary, "Ultra-wideband (UWB) incidence on multiple dielectric interfaces," in *Proc. IEEE Antennas Propag. Soc. Symp.*, 2004, pp. 1315–1318.

[139] A. Muqaibel, A. Safaai-Jazi, A. Bayram, and S. Riad, "UWB through-the-wall propagation and material characterization," in *Proc. IEEE Antennas Propag. Soc. Int. Symp.*, 2003, pp. 623–626.

[140] R. Yao, Z. Chen, and Z. Guo, "An efficient multipath channel model for uwb home networking," in *Proc. IEEE Radio Wireless Conf.*, 2004, pp. 511–516.

[141] R. M. Buehrer, W. A. Davis, A. Safaai-Jazi, and D. Sweeney, "Ultra wideband propagation measurements and modeling—Final report to DARPA NETEX program," Virginia Tech, Blacksburg, Tech. Rep., 2004.

[142] J. Y. Lee and S. Choi, "Through-material propagation characteristic and time resolution of UWB signal," in *Proc. IEEE UWBST*, 2004, pp. 71–75.

[143] M. Di Renzo, M. Feliziani, F. Graziosi, G. Manzi, and F. Santucci, "Characterization of the ultra-wide band channel," in *IEEE Int. Conf. Wireless Commun. Appl. Computat. Electromagn.*, 2005, pp. 27–30.

[144] R. C. Qiu, C. Zhou, and Q. Liu, "Physics-based pulse distortion for ultra-wideband signals," *IEEE Trans. Veh. Technol.*, vol. 54, pp. 1546–1555, 2005.

[145] W. Zhang, T. D. Abhayapala, and J. Zhang, "UWB spatia—Frequency channel characterization," in *Proc. Veh. Technol. Conf. Spring 2006*, 2006.

[146] W. Q. Malik, C. J. Stevens, and D. J. Edwards, "Spatio-temporal ultrawideband indoor propagation modelling by reduced complexity geometric optics," *IET Commun.*, vol. 1, no. 4, pp. 751–759, Aug. 2007.

[147] K. W. Lam, Q. Li, L. Tsang, K. L. Lai, and C. H. Chan, "On the analysis of statistical distributions of UWB signal scattering by random rough surfaces based on Monte Carlo simulations of Maxwell equations," *IEEE Trans. Antennas Propag.*, vol. 52, 2004.

[148] R. Vaughan and J. B. Andersen, *Channels, Propagation and Antennas for Mobile Communications*. London, U.K.: IEE Press, 2003.

[149] Y. Wang, S. Safavi-Naeini, and S. Chaudhuri, "A hybrid technique based on combining ray tracing and fdtd methods for site-specific modelling of indoor radio wave propagation," *IEEE Trans. Antennas Propag.*, vol. 48, pp. 743–754, 2000.

[150] M. Porebska, T. Kayser, and W. Wiesbeck, "Verification of a hybrid ray-tracing/fdtd model for indoor ultra-wideband channels," in *Proc. 10th Eur. Wireless Technol. Conf.*, Munich, Germany, 2007.

[151] A. Domazetovic, L. J. Greenstein, N. B. Mandayam, and I. Seskar, "A new modeling approach for wireless channels with predictable path geometries," in *Proc. VTC 2003 Fall*, 2003, pp. 454–458.

[152] A. F. Molisch, J. R. Foerster, and M. Pendergrass, "Channel models for ultrawideband personal area networks," *IEEE Wireless Commun.*, vol. 10, pp. 14–21, Dec. 2003.

[153] J. R. Foerster, "Channel modeling sub-committee report final," Tech. Rep. P802.15 02/490r1, IEEE 802.15 SG3a, Feb. 2003.

[154] M. Pendergrass and W. C. Beeler, "Empirically based statistical ultra-wideband (UWB) channel model," Tech. Rep. P802.15 02/240SG3a, 2002, IEEE P802.15 SG3a contribution.

[155] J. Zhang, P. V. Orlik, Z. Sahinoglu, A. F. Molisch, and P. Kinney, "UWB systems for wireless sensor networks," *Proc. IEEE*, vol. 97, no. 2, Feb. 2009.

[156] K. Siwiak, H. Bertoni, and S. M. Yano, "Relation between multipath and wave propagation attenuation," *Electron. Lett.*, vol. 39, no. 1, pp. 142–143, Jan. 2003.

ABOUT THE AUTHOR

Andreas F. Molisch (Fellow, IEEE) received the Dipl.Ing., Dr.Techn., and habilitation degrees from the Technical University Vienna (Austria) in 1990, 1994, and 1999, respectively. From 1991 to 2000, he was with the TU Vienna, becoming an associate professor there in 1999. From 2000–2002, he was with the Wireless Systems Research Department at AT&T (Bell) Laboratories Research in Middletown, NJ. From 2002–2008, he was with Mitsubishi Electric Research Labs, Cambridge, MA, USA, most recently as Distinguished Member of Technical Staff and Chief Wireless Standards Architect. Concurrently he was also Professor and Chairholder for radio systems at Lund University, Sweden. Since 2009, he is Professor of Electrical Engineering at the University of Southern California, Los Angeles, CA, USA.

Dr. Molisch has done research in the areas of SAW filters, radiative transfer in atomic vapors, atomic line filters, smart antennas, and wideband systems. His current research interests are measurement and modeling of mobile radio channels, UWB, cooperative communications, and MIMO systems. Dr. Molisch has authored, co-authored or edited four books (among them the textbook *Wireless Communications*, Wiley-IEEE Press), eleven book chapters, more than 110 journal papers, and numerous conference contributions, as well as more than 70 patents.

Dr. Molisch is an editor of the IEEE TRANSACTIONS ON WIRELESS COMMUNICATIONS and co-editor of special issues of several journals. He has been member of numerous TPCs, vice chair of the TPC of VTC 2005 spring, general chair of ICUWB 2006, TPC co-chair of the wireless symposium of Globecomm 2007, TPC chair of Chinacom 2007, and general chair of Chinacom 2008. He has participated in the European research initiatives "COST 231," "COST 259," and "COST 273," where he was chairman of the MIMO channel working group, he was chairman of the IEEE 802.15.4a channel model standardization group. From 2005–2008, he was also chairman of Commision C (signals and systems) of URSI (International Union of Radio Scientists) and since 2009, he is the Chair of the Radio Communications Committee of the IEEE COMMUNICATIONS SOCIETY. Dr. Molisch is a Fellow of the IEEE, a Fellow of the IET, an IEEE Distinguished Lecturer, and recipient of several awards.